HHS Public Access

Author manuscript

J Immunol. Author manuscript; available in PMC 2018 July 01.

Published in final edited form as:

J Immunol. 2017 July 01; 199(1): 348–362. doi:10.4049/jimmunol.1601494.

Comprehensive approach for identifying the T-cell subset origin of CD3 and CD28 antibody-activated chimeric antigen receptor-modified T-cells

Michael Schmueck-Henneresse[*,†,‖], **Bilal Omer**[‖,$], **Thomas Shum**[‖,%], **Haruko Tashiro**[‖], **Maksim Mamonkin**[‖], **Natalia Lapteva**[‖], **Sandhya Sharma**[‖,%], **Lisa Rollins**[‖], **Gianpietro Dotti**[‖], **Petra Reinke**[†,‡], **Hans-Dieter Volk**[*,‡], and **Cliona M. Rooney**[‖,*,#,^]

[*]Institute for Medical Immunology, Charité University Medicine Berlin, Germany

[†]Department of Nephrology and Internal Intensive Care, Renal and Transplant Research Unit, Charité University Medicine Berlin, Germany

[‡]Berlin-Brandenburg Center for Regenerative Therapies (BCRT), Charité University Medicine Berlin, Germany

[‖]Center for Cell and Gene Therapy, Baylor College of Medicine, The Methodist Hospital, Texas Children's Hospital, Houston, Texas, USA

[$]Department of Pediatrics, Division of Hematology and Oncology, Baylor College of Medicine

[#]Departments of Molecular Virology and Microbiology, Baylor College of Medicine

[^]Department of Pathology, Baylor College of Medicine

[%]Department of Graduate Program of Translational Biology and Molecular Medicine, Baylor College of Medicine

Abstract

The outcome of therapy with CAR-modified T-ells is strongly influenced by the subset origin of the infused T-cells. However, since polyclonally activated T-cells acquire a largely $CD45RO^{+}CCR7^{-}$ effector memory phenotype after expansion, regardless of subset origin, it is impossible to know which subsets contribute to the final T-cell product. To determine the contribution of naïve (T_{naive}), memory stem (T_{SCM}), central memory (T_{CM}), effector memory (T_{EM}) and terminally differentiated effector (T_{EMRA}) T-cell populations to the CD3 and CD28-activated CAR-T-cells that we use for therapy, we followed the fate and function of individually

Corresponding author: Michael Schmueck-Henneresse, Charité University Medicine Berlin, Institute for Medical Immunology and BCRT, Augustenburger Platz 1, D-13353 Berlin, Germany, phone: +49 (0)30 450 539495, fax: +49 (0)30 450 524932, michael.schmueck-henneresse@charite.de.

Disclosures

CMR is on the scientific advisory board of Cell Medica.

Author contributions

M.S.-H. led the project, designed the research, performed most of the experiments, analyzed and interpreted the data, and significantly contributed to writing of the manuscript. C.M.R designed the research, interpreted the data, and significantly contributed to writing of the manuscript. P.R. and H.-D.V. helped to design the research. B.O., T.S., H.T. helped to design the experiments, performed some of the experiments and helped to analyze data. M.M. and N.L. helped to design the experiments. S.S. and L.R. provided technical assistance. G.D. provided the CAR constructs and helped to design the experiments.

sorted CAR-T-cell subsets after activation with CD3 and CD28 antibodies (CD3/28), transduction and culture alone or after reconstitution into the relevant subset-depleted population. We show that all subsets are sensitive to CAR transduction and each developed a distinct T-cell functional profile during culture. Naïve-derived T-cells showed the greatest rate of proliferation but had more limited effector functions and reduced killing than memory-derived populations. When cultured in the presence of memory T-cells, naïve-derived T-cells show increased differentiation, reduced effector cytokine production, and a reduced re-proliferative response to CAR stimulation. CD3/28-activated T-cells expanded in IL-7 and IL-15 produced greater expansion of T_{SCM}- and T_{CM}-derived T-cells compared to IL-2. Our strategy provides a powerful tool to elucidate the characteristics of CAR T-cells, regardless of the protocol used for expansion, reveals the functional properties of each expanded T-cell subset and paves the way for a more detailed evaluation of the effects of manufacturing changes on the subset contribution to *in vitro* expanded T-cells.

Introduction

Adoptive T-cell immunotherapy with CAR-modified T-cells (CAR-T-cells) targeting tumor antigens have been incorporated into cancer treatment with promising efficacy in distinct settings (1–4). CARs are genetically engineered immunoreceptors comprising a single-chain antibody fragment (scFv) linked to cytosolic endodomains from costimulatory receptors and/or the T-cell receptor (TCR)ζ chain (5–7). The structure of the CAR, including the affinity of the scFv, the type of spacer and costimulatory endodomains, the design of the clinical protocol and the disease targeted profoundly affect the fate and function of CAR T-cells, as does the manufacturing protocol that determines the character of the T-cell product infused. (2–4, 8–23). Data regarding the best T-cell subset from which to derive CAR T-cells for infusion are inconclusive and controversial and most patients receive $CD4^+$ and $CD8^+$ T-cells whose subset derivation is unknown (2–4, 11–20). The ultimate objective of T-cell therapy is to transfer a long-lived T-cell population with the capacity to differentiate into potent tumor-specific effectors and to self-renew (8, 24). Short-lived effector T-cells (T_{EFF}) possess potent effector function *in vitro*, however, appear less attractive for adoptive immunotherapy because of their limited proliferation and engraftment *in vivo* (25–27). Memory T-cells subsets have been shown to expand substantially *in vivo* and are long-lived with their self-renewal capacity being inversely proportional to their differentiation state (28). Recently, it has been reported that antigen-experienced memory T-cell subsets directly promote the phenotypic and functional differentiation of naïve T-cells, which as a consequence lost anti-tumor potential when transferred *in vivo* (29).

Expression of the lymph node homing molecules CCR7 and the leucocyte common antigen (CD45) isoforms RA and RO distinguishes memory from naïve T-cells and allows the dissection of the memory/effector T-cell compartment at least into four main subsets (30, 31): Memory stem T-cells (T_{SCM}), central memory T-cells (T_{CM}), effector memory (T_{EM}) and terminally differentiated effector T-cells (T_{EMRA}) (24, 30, 31). T_{CM} co-express CCR7 and CD45RO, having lost CD45RA during naïve → memory transition (32). Upon antigenic restimulation T_{CM} lose CCR7 expression and differentiate into T_{EM} (32, 33) and finally into $T_{EMRA,}$ which are considered to be terminally differentiated. T_{EMRA} lack both CCR7 and CD45RO and re-express CD45RA (34). A 4^{th} memory subset T_{SCM} resides

phenotypically within the naïve-like T-cell compartment ($CD45RO^{-}CD45RA^{+}CCR7^{+}$), distinct from naïve T-cells by their expression of CD95 (Fas) (24, 31). Each T-cell subset has distinct engraftment capacities and function following adoptive transfer in preclinical trials (31–33, 35). In particular, T_{CM} are thought to have superior engraftment and persistence compared to more differentiated memory T-cell subsets (24, 28, 30–33, 35–39). The recently described T_{SCM} subset may represent the earliest stage of memory T-cell differentiation and may have the ability to transfer stem cell-like T-cells for improved long-term efficacy (40, 41).

To identify the characteristics and subset derivation of CAR T-cells polyclonally expanded on CD3 and CD28 antibody-coated plates as used in our clinical studies (2–4, 11–20), we sorted each T-cell subset and followed its fate and function after activation, CAR-transduction and culture alone and after reconstitution into the corresponding subset-depleted, polyclonally activated bulk peripheral blood mononuclear cells (PBMC). In a proof-of-concept study, we demonstrate that each T-cell subset is sensitive to CAR transduction, and each displays a specific functional profile. Naïve T-cell-derived populations showed the most rapid expansion and dominated the cultures by the end of the culture period, but had reduced effector functions and killing compared to memory subsets. Furthermore, T_{naive}-derived cells cultured in the presence of memory T-cells differentiate more than when cultured alone, and show coincidentally reduced effector cytokine production and ability to proliferate in response to CAR stimulation. T_{SCM} show the most rapid expansion of all subsets, but due to their low frequency at the start of culture, they represented only a minor fraction at the end. Finally we found that compared to IL-2, a combination of IL-7 and IL-15, increased the yield of T_{SCM} and T_{CM} derived T-cells within the bulk cultures. Irrespective of the protocol used for expansion, our comprehensive approach reveals the characteristics of CAR T-cells polyclonally expanded from PBMC, demonstrates the functional properties of each expanded T-cell subset and underlines the importance of culture conditions to influence the desired T-cell populations. To this end, our strategy allows a meticulous assessment of the effects of manufacturing changes on the subset contribution to *in vitro* expanded T-cells.

Materials and Methods

Cell culture

All PBMC and T-cell cultures and all assays were performed using complete media (45% RPMI 1640 (Hyclone, CA, USA), 45% Click's (Irvine, CA, USA)) supplemented with 5mM L-glutamine (Invitrogen, Carlsbad, CA), penicillin (100IU/ml), and streptomycin (Hyclone, Logan, UT), containing 10% fetal bovine serum (Hyclone), in humidified incubators at 37°C and 5% CO_2.

Blood samples

For all experiments, blood samples were collected with informed consent from healthy volunteers on protocols approved by the Baylor College of Medicine Institutional Review Board (IRB). Peripheral blood mononuclear cells were isolated from blood by lymphoprep density gradient centrifugation (Stem Cell Technologies, Vancouver, BC).

T cell isolation and sorting

PBMCs were enriched for $CD3^+$ T-cells with the pan T-cell "untouched" Isolation Kit II (Miltenyi Biotech) following the manufacturer's instructions. Cells were labeled with fluorescent antibodies to CD3, CD45RO, CD95, CCR7 (all purchased from Biolegend) and CD45RA (Beckman Coulter). FACSorting was performed for T_{CM} ($CCR7^+CD45RA^-$), T_{EM} ($CCR7^-CD45RA^-$), T_{EMRA} ($CCR7^-CD45RA^+$), T_{SCM} ($CD45RA^+CCR7^+ \rightarrow CD95^+$) and T_{naive} ($CD45RA^+CCR7^+ \rightarrow CD95^-$) (24, 30, 42) on a BD FACSAriaII SORP (BD Biosciences). Postsorting analysis of purified subsets revealed greater than 98% purity.

Cell lines

NIH 293T, JEKO and HDLM-2 cell lines (ATCC city state) were cultured in IMDM (BioWhittaker, Walkersville, MD) supplemented with 10% FCS (Hyclone, Logan, UT) and 5 mM L-glutamine (Thermo Fisher, Waltham, MA). 2^{nd} generation GD2.CAR (14g2a.CD28ζ CAR) transduced T-cells were directed to the disialoganglioside (GD2) to assess specific *in vitro* re-expansion and effector function. Expanded 2^{nd} generation $CD19.CAR^+$ (FMC63.CD28ζ CAR) and $CD19.CAR\text{-}NGFR^+$ (FMC63.CD28ζ-I-NGFR CAR) T-cells were analyzed for their ability to produce cytokines in response to CAR-antigen-expressing target cells, which constituted JEKO ($CD19^+$) and HDLM-2 ($CD19^-$) cell lines.

Constructs

We used CAR constructs directed to the disialoganglioside, GD2, and the B-cell marker, CD19, that have been targeted in many clinical studies. 2^{nd} generation GD2.CAR (14g2a.CD28-ζ) and the CD19.CAR (FMC63.CD28ζ) cloned into SFG vectors have previously been described (43–45). The CD19.CAR construct was used alone and or cloned upstream of an IRES-NGFR or IRES mOrange to facilitate selection and detection.

Retroviral supernatant

Transient retroviral supernatants were produced by co-transfection of NIH 293T cells with the MoMLV gag/pol expression plasmid PeqPam3(-env), the RD114(-env) expression plasmid RDF, and SFG vectors at a ratio of 3:2:3, respectively, with a total of 10μg DNA. The transfection was facilitated with GeneJuice reagent (Calbiochem). The supernatant was harvested 2 and 3 days after transfection, filtered (using a 0.45μm filter), snap-frozen, and stored at −80°C in 5mL aliquots.

Cell stimulation and expansion

PBMC or FACSorted T-cells were activated on CD3 (from the OKT3 hybridoma: ATCC #CRL 8001, Manassas, VA) and CD28 (Becton Dickinson BD, Franklin Lakes, NJ) antibody-coated plates at (500 μL of 1μg/mL each in the presence of recombinant human (rh) IL-2 (50IU/mL) or rhIL-7 and rhIL-15 (each at 10ng/mL). In some experiments, CD3/28 antibody-activated subsets were transduced on day 2 after activation, then reconstituted into CD3/28-activated T_{SUBSET}-depleted PBMC on day 3 of culture at their initial frequency or cultured separately. The medium and cytokines were changed every 3 days during culture or when passaging the T-cells for splitting during expansion.

Transduction

T cells or T-cell subsets were transduced 2 days after activation: Non-tissue-treated 24-well plates were coated with 500μL 1mg/mL retronectin (Takara Biochemicals, Shiga, Japan) overnight. After removing the retronectin, 1.5 – 2mL of retroviral supernatant was added per well and centrifuged at 2000 × g for 1 hr at 25°C to allow vector adherence. The supernatant was removed prior to the addition of CD3/28 activated peripheral blood derived T-cells or FACSorted T-cell subsets. Cells were incubated for 2 days on the virus-coated plate in the presence of 50IU/ml rhIL-2 (Proleukin, Chiron Corp., Emeryville, CA, USA) or 10ng/mL rhIL-7 and 10ng/mL rhIL-15 (Peprotech), then transferred to tissue-culture-treated plates. Where indicated, one day after transduction, each T_{SUBSET} was reconstituted at its initial frequency into the corresponding subset-depleted population.

Flow cytometry, antibodies and intracellular staining

Following antigen specific stimulation, cytokine production (IFNγ, TNFα, IL-2) was determined by intracellular fluorescence staining. All antibodies were purchased from Biolegend, unless indicated otherwise. $GD2^+$ JF cell lines (serving as stimulator cells for 2^{nd} generation GD2.CAR T-cells) and $CD19^+$ JEKO cell lines (serving as stimulator cells for 2^{nd} generation CD19.CAR T-cells) were added to T-cells at a stimulator to responder ratio of 10:1. HDLM-2 cells lack GD2 and CD19 were used as controls and respective background responses have been subtracted from CAR-specific cytokine production. For effector cytokine detection, cultured T-cells were re-stimulated for 6 hrs in the presence of 1μg/mL brefeldin A (BFA; Sigma-Aldrich). After harvesting, phenotype staining was performed using monoclonal antibodies for CD3 (OKT3), CD4 (SK3) and CD8 (RPA-T8). To define memory subsets, T-cells were extracellularly stained for CCR7 (G043H7), CD45RA (HI100), CD45RO (UCHL1) and CD95 (DX2). In particular experiments a αNGFR (C40-1457, BD) antibody was used to stain for NGFR expression on CD19.CAR-$NGFR^+$ T-cells. Transduction efficacies were assessed by staining for the CAR expression on the T-cell surface utilizing antibodies targeting GD2 (IA7) (46) or CD19.CAR (goat anti-human-IgG (H+L)) (Jackson ImmunoResearch, West Grove, PA). To exclude dead cells, live/dead-discrimination staining-dye (Invitrogen) was added. Subsequently, cells were permeabilized with Perm2 solution (BD Biosciences) and stained for IFNγ (4S.B3), TNFα (MAb11), and IL-2 (MQ1-17H12). Cells were analyzed on a LSR-II flow cytometer and FlowJo Version 10 software (Tree Star). Lymphocytes were gated based on the FSC versus SSC profile and subsequently gated on FSC (height) versus FSC to exclude doublets.

Assessment of cytotoxic activity

A modified *vital assay* was used for cytotoxicity testing as described previously (24, 47, 48). Briefly, the JEKO cell line served as a CD19-positive target cell for 2^{nd} generation CD19.CAR T-cells, while HDLM-2 cells that lack CD19 were used as control targets. JEKO cells were labeled with 10μM carboxyfluorescein succinimidyl-ester (CFDA-SE; Molecular Probes). As controls, $CD19^-$ HDLM-2 were labeled with 5μM dimethyldodecylamine oxide-succinimidyl-ester (DDOA; Invitrogen). Cells were co-cultured in duplicate for 16 hrs in T-cell / target cell ratio of 1:1 and 10:1. Labeled cells were analyzed as duplicates using LSR-II flow cytometer. Samples without T-cells, containing only targets and non-targets

(CD19$^+$ JEKO cell lines or CD19$^-$ HDLM-2) displayed as internal controls. Cells were gated using live/dead-discrimination staining-dye negative cells (Invitrogen). The mean percent survival of CD19$^+$ JEKO target cells was calculated relative to CD19$^-$ HDLM-2 controls. Percentage target cell lysis was calculated as follows: mean percent survival of targets in cultures containing defined numbers of effector T-cells in comparison to control cells without T-cells.

Statistical analysis and calculations

Statistical analysis was performed with GraphPad Prism version 6. Data were analyzed using repeated measures 1-way ANOVA, 2-way ANOVA or paired t-test as indicated, after verifying Gaussian distribution with the Kolmogorov-Smirnov test. p-values ≤ 0.05 were considered significant: *p<0.05, **p<0.01, ***p<0.001. T-cell subset fold expansion expresses T-cell subset numbers (assessed by FACS) in relation to total cell numbers of the indicated days post-initial stimulation and day 1.

Results

Comparative proliferation of isolated T-cell subsets cultured alone

To analyze the characteristics of each T-cell subset transduced with a GD2.CAR we compared their proliferation and phenotype following CD3/28 antibody activation (in the presence of IL-7 and IL-15) and cytokine production following stimulation via the CAR using the CAR antigen (diasialoganglioside: GD2). First CD3$^+$ T-cells were enriched from PBMC by magnetic bead sorting, then T_{CM} (CCR7$^+$CD45RA$^-$), T_{EM} (CCR7$^-$CD45RA$^-$), T_{EMRA} (CCR7$^-$CD45RA$^+$), T_{SCM} (CD45RA$^+$CCR7$^+$→CD95$^+$) and T_{naive} (CD45RA$^+$CCR7$^+$→CD95$^-$) were isolated by polychromatic fluorescence-activated cell sorting (FACSorting) (Fig. 1A). The average frequency of each T-cell subset from pre-sorted CD3$^+$ T-cells was 21.5±6.2% for T_{CM}, 17.8±8.8% for T_{EM}, 9.8±5.5% for T_{EMRA}, 0.9±0.2% for T_{SCM} and 50.5±9.2% for T_{naive} (Fig. 1B). To determine if all T-cell subsets isolated from PBMC were sensitive to retroviral transduction, we transduced each subset with a 2nd generation CAR (14g2a.CD28-ζ) targeting GD2 (43) on day 2 after stimulation.

As presented in Figure 1C, the GD2.CAR could be expressed in all T-cell subsets with median transduction efficacies of 60.2±10.2%, 60.1±7.2%, 66.6±7.9%, 61.2±7.1% and 64.6±6.1% for CD4$^+$ T_{PBMC}, T_{CM}, T_{EM}, T_{EMRA}, T_{naive} and 65.6±20.7%, 70.8±15.4%, 75.3±12.3%, 61.7±16.8%, 66.6±19.2% and 82.7±7.9% in CD8$^+$ T_{PBMC}, T_{CM}, T_{EM}, T_{EMRA}, T_{SCM}, T_{naive}, respectively (summarized in Fig. 2A). We observed a trend towards higher transduction efficacies in CD8$^+$ compared with CD4$^+$ T-cells (62.5% in CD4$^+$ T-cells and 70.4% in CD8$^+$ T-cells) (Fig. 2A). As shown in Figure 2B, we detected a preferential expansion of CD8$^+$ T-cells compared to CD4$^+$ T-cells within T_{PBMC}, T_{CM}, T_{EM}, T_{EMRA}, T_{SCM}, but not in T_{naive} populations. As previously reported for T_{SCM}-derived cells (24), we observed almost exclusive proliferation of CD8$^+$ T_{SCM}, whereas CD4$^+$ T_{SCM} expansion could not be detected. However, all other expanded T-cell subsets showed a balanced CD4$^+$ / CD8$^+$ ratio (Fig. 2A, B). When cultured individually, all T-cell subsets proliferated in response to CD3/28 stimulation, confirming their viability after separation and all transduced T-cell subsets showed rapid expansion with the highest expansion at day 14 from

T_{SCM}-derived (311±63 fold) followed by T_{naive}-derived (210±24 fold), T_{CM}-derived (150±65 fold), and lower expansion of T_{EM}-derived (88±31 fold), and T_{EMRA}-derived (61±22 fold) cells (Fig. 2C). All transduced subsets differentiated during culture so that by day 14, $CCR7^{-}CD45RO^{+}$ T_{EM} cells predominated in T_{EMRA}- and T_{EM} –derived subsets, whereas a substantial proportion of $CCR7^{+}CD45RO^{+}$ T_{CM} cells was present in T_{CM}-, T_{naive}- and T_{SCM}-derived cultures (Fig. 2D), demonstrating that naïve T-cells develop a memory phenotype in response to CD3/28 stimulation *in vitro*.

Cytokine production and proliferation of $T_{SUBSETS}$ in response to CAR stimulation

To examine CAR-specific effector functions, we stimulated each transduced subset on day 14 with the GD2-positive JF neuroblastoma cell line and a GD2-negative Hodgkin lymphoma (HDLM2) and measured IFNγ cytokine expression in intracellular cytokine assays (Fig. 2E). GD2-specific IFNγ production from $CD4^{+}$ and $CD8^{+}$ T_{CM}-, T_{PBMC}- and T_{SCM}-derived cells was greater than from T_{naive}-, T_{EMRA}- and T_{EM}-derived cells. No IFNγ was produced by non-transduced T-cells in response to JF cells (data not shown). To compare T-cell subset proliferation in response to CAR stimulation each transduced subset was stimulated with plate bound GD2 (used to avoid tumor-derived activating or inhibitory signals) in the absence of exogenous cytokines on day 14 of culture. Intriguingly, T_{EMRA}- and T_{naive}-derived cells failed to proliferate, whereas T_{SCM}-, T_{CM}- and T_{EM}-derived cells showed robust re-expansion in response to CAR antigen over 7 days of culture (Fig. 2F). However, T_{naive}-derived cells did proliferate (18-fold expansion) when IL-7 and IL-15 were added to the re-expansion culture (data not shown) indicating greater dependence on exogenous cytokines than memory-derived T-cells.

In summary, all tested T-cell subsets were susceptible to CAR transduction and expanded when activated via the TCR with greatest fold expansion by T_{SCM}- > T_{naive}- > T_{CM}- > T_{EM}- > T_{EMRA}-derived cells. While lower in T_{EM}- and T_{EMRA}-derived cells, all subsets produced IFNγ following CAR-stimulation and acquired a memory T-cell phenotypic profile. T_{SCM}-, T_{CM}- and T_{EM}-derived cells showed a greater capacity to expand in response to CAR stimulation than T_{EMRA}- and T_{naive}-derived cells.

Naïve derived T-cells expand preferentially within polyclonally activated PBMC but show reduced effector cytokine production and killing

To evaluate the characteristics of each T-cell subset when reconstituted into the bulk subset-depleted PBMC population, each T-cell subset was purified from PBMC by FACS (Fig. 3A, B) then activated with CD3 and CD28 antibodies and transduced with a retroviral vector encoding both a 2nd generation CD19.CD28ζ CAR and a truncated *nerve growth factor receptor* (NGFR) (CD19.CAR-NGFR) separated by an IRES to allow flow-cytometric detection following expansion. In parallel, each subset-depleted PBMC population was CD3/28-activated and transduced with the same 2nd generation CD19.CAR, but without NGFR (Fig. 3C, D). One day after transduction, each T_{SUBSET} was reconstituted at its initial frequency into the corresponding subset-depleted population. This design allowed us to distinguish the depleted bulk transduced PBMC from the reconstituted transduced T-cell subset by flow cytometric detection of NGFR (Fig. 3D). All T-cell subsets were sorted to greater than 98% purity as shown in Figure 3B and 3C and transduced with frequencies

exceeding 80% (Fig. 3E). CD19.CAR transduction did not affect the survival or expansion of any T-cell subset compared to non-transduced subsets cultured alone in parallel (data not shown).

Differences in the rate of proliferation of each transduced subset cultured alone or within the transduced bulk population could not be detected (Fig. 4A). However, the rate of expansion of T-cell subsets within the bulk culture was much greater for T_{naive}- ($CD3^+$ 234±36 fold expansion) and T_{SCM}-derived cells ($CD3^+$ 621±189 fold expansion) than for T_{EMRA}- and T_{EM}-derived cells ($CD3^+$ 44±6 and 54±9 fold expansion), while T_{CM}-derived cells showed an intermediate rate of expansion ($CD3^+$ 204±48 fold expansion) (Fig. 4A), so that by day 14 T_{naive}-derived cells dominated the cultures (76±19% of $CD3^+$ T-cells) with T_{CM}-derived cells comprising a mean of 30±12% of $CD3^+$ T-cells (Fig. 4B, C). $CD4^+$ and $CD8^+$ T_{EMRA}- and T_{EM}-derived cells could barely be detected because of the other more rapidly expanding subsets (Fig. 4B, C). Hence, bulk CD3/28-activated T-cells were derived almost entirely from naïve $CD8^+$ T-cells and naïve and T_{CM} $CD4^+$ T-cells, with little or no contribution from T_{EM} and T_{EMRA} subsets (Fig. 4B, C). Of note, despite their high rate of expansion when cultured in bulk PBMC, T_{SCM}-derived cells represented less than 2% of the bulk cultures on day 14 because of their low starting frequency.

By day 14 of culture, T-cells with a T_{EM} phenotype ($CCR7^-CD45RO^+$) dominated all subset derived-cultures (Supplemental Fig. 1A, B). However a substantial proportion of T-cells with a T_{CM} phenotype could be detected within expanded T_{CM}- (CD4+ 20.4±2.9%; CD8+ 13.5±2.6%), T_{naive}- ($CD4^+$ 45.2±6.9%; $CD8^+$ 18.5±2.4%) and CD8+ T_{SCM}-derived cells (19.4±2.7%) as well as in bulk PBMCs-derived cells ($CD4^+$ 12.4±2.8%; $CD8^+$ 15.7±3.9%).

To evaluate cytokine production in response to CAR stimulation by T-cell subset-derived cells expanded within bulk PBMC, we performed intracellular flow and co-stained with antibodies to NGFR (the marker for the subset) and to the spacer/hinge region of the CD19.CAR (Fig. 5A, B) to distinguish subset- and bulk-derived T-cells. Figures 5C–D show IFNγ, TNFα and IL-2 production from each T-cell subset ($CD4^+$: red- $CD8^+$ blue bars) and from the T-cell subset-depleted bulk population ($CD4^+$: black- $CD8^+$ white bars) in response to a $CD19^+$ mantle cell lymphoma (JEKO) and a $CD19^-$ Hodgkin lymphoma (HDLM2). T_{naive}-derived cells produced relatively low levels of all cytokines compared to bulk-derived T-cells and to other subsets, which showed similar capacities to produce cytokines in response to CAR stimulation, even when their frequencies within the co-cultures were low (Fig. 5C, D and E).

We next tested the killing capacity of each subset cultured alone and its respective subset-depleted and subset-reconstituted PBMC cell preparation (Fig. 6A). Figure 6B shows the killing capacity of each T-cell subset cultured alone, T-cell subset-depleted bulk population and T-cell subset-reconstituted bulk population in response to a $CD19^+$ mantle cell lymphoma (JEKO) and a $CD19^-$ Hodgkin lymphoma (HDLM2). Intriguingly, killing of $CD19^+$ JEKO was significantly reduced in cultures where T_{CM} and T_{EM} were depleted from the bulk PBMC population (Fig. 6B upper panel). By contrast T-cell subset-reconstituted populations showed little variance in their killing (Fig. 6B middle panel). Comparison of the

T-cell subsets cultured alone revealed a significantly lower killing capacity of T_{naive}-derived cells (Fig. 6B lower panel).

In summary, T_{naive}-derived cells expand preferentially within polyclonally activated PBMC, express a memory T-cell surface marker profile but show reduced effector cytokine production and killing compared to memory-derived subsets.

Naïve derived T-cells show increased differentiation when cultured in the presence of bulk (memory) T-cells and show reduced effector cytokine production and re-expansion capacity in response to CAR stimulation

To evaluate the phenotypic and functional characteristics of each T-cell subset cultured in the presence of the whole PBMC preparation compared to T-cells cultured alone, we followed the experimental setup presented earlier, comprising the transduction of each T-cell subset using a retroviral vector encoding both a 2nd generation CD19.CD28ζ CAR and a truncated NGFR (CD19.CAR-NGFR) and in parallel transduction of each subset-depleted PBMC population with the same 2nd generation CD19.CAR, but without NGFR. Initially, we followed the fate of individually sorted CAR-transduced T-cell subsets after activation, transduction and culture alone or after reconstitution into the relevant subset-depleted population (Fig. 7A). Each T-cell subset differentiated during culture and by day 7 of culture T-cells with T_{CM} and T_{EM} phenotypes ($CCR7^+CD45RO^+$ and $CCR7^-CD45RO^+$, respectively) dominated all subset-derived cultures (Fig. 7A, B). We defined the T_{CM} proportion of each T-cell subset as a measure of differentiation. When comparing the phenotype of each transduced subset cultured alone or within the transduced bulk PBMC population we found significantly higher proportions of phenotypically less-differentiated T_{CM} cells in separately cultured T_{CM}- and T_{naive}-derived cells (day 14: T_{CM}-derived cells cultured in bulk: $CD4^+$ 13.1±2.6%; $CD8^+$ 12.9±1.4% versus T_{CM}-derived cells cultured alone: $CD4^+$ 21.7.1±9.9%; $CD8^+$ 21.2±5.4% and T_{naive}-derived cells cultured in bulk: $CD4^+$ 14.8±4.7%; $CD8^+$ 11.2±1.1% versus T_{naive}-derived cells cultured alone: $CD4^+$ 39.8±7.8%; $CD8^+$ 29.1±6.6%) (Figure 7A, B). A substantial proportion of T-cells with a T_{CM} phenotype could also be detected within expanded $CD8^+$ T_{SCM}-derived cells (day 14: T_{SCM}-derived cells cultured in bulk: 15.3±1.7% versus T_{SCM}-derived cells cultured alone: 22.6±0.9%)(Fig. 7A, B). Of note, T-cell cultures derived from less-differentiated T_{SCM}-, T_{CM}- and T_{naive} had more stable CAR expression in long-term cultures up to day 21, whereas T_{EM}- and T_{EMRA}-derived cultures showed partial loss of their CAR (Supplemental Fig. 2).

When comparing intracellular cytokine production in response to CAR stimulation (using the $CD19^+$ mantle cell lymphoma: JEKO) of each transduced subset cultured alone or within the transduced bulk PBMC population, T_{naive}-derived cells produced less IFNγ when cultured within the transduced bulk PBMC population than when cultured alone, whereas all other subsets showed similar capacity of IFNγ production, regardless of whether cells were cultured in the presence of the whole PBMC preparation or alone (Supplemental Fig. 3). T_{naive}-derived cells produced relatively low levels of IFNγ compared to other T-cell subsets that produced similar cytokine levels in response to CAR stimulation (Supplemental Fig. 3).

Finally, we compared T-cell subset proliferation in response to CD19.CAR stimulation. Each transduced subset cultured alone or T-cell subset-derived cells expanded within bulk PBMC was stimulated on day 14 of culture using $CD19^+$ JEKO cells in the presence or absence of exogenous cytokines (IL-7 and IL-15) (Fig. 8A) and fold T-cell subset expansion was measured 7 days later. To assess the expansion of each subset cultured in the presence of the whole PBMC preparation, we used antibodies to NGFR (T-cell subset) and to the spacer/hinge region of the CD19.CAR before and after CAR stimulation (Fig. 8A). In the absence of exogenous cytokines T_{EMRA}- and T_{naive}-derived cells failed to proliferate, whereas T_{SCM}-, T_{CM}- and T_{EM}-derived cells expanded to a similar degree regardless of whether cultured alone or within the transduced bulk population (Fig. 8B). When culture with cytokines, only T_{EMRAs} did not expand. As expected the expansion of the remaining subsets was much greater than without cytokines (Fig. 8C), and notably, T_{naive}-derived cells showed significantly greater expansion when cultured alone than when cultured within the transduced bulk population (65-fold for $CD4^+$ and 36-fold for $CD8^+$ alone compared to 43-fold for $CD4^+$ and 15-fold for $CD8^+$ cultured in bulk) (Fig. 8C). In contrast, all other subsets showed slightly greater expansion when cultured in bulk (Fig. 8C).

In summary, T_{naive}-derived cells differentiate more when cultured in the presence of memory T-cells than when cultured alone, and show coincidentally reduced effector cytokine production and re-expansion capacity in response to CAR stimulation. Overall, T_{naive}-derived cells show reduced effector cytokine production compared to memory-derived subsets, and lack the ability to respond to stimulation in the absence of cytokines.

The yield of T_{SCM}- and T_{CM}-derived T-cells is increased by culture in IL-7 with IL-15, compared to culture in IL-2

Because the T_{naive}-derived CAR-cells that dominated our cultures showed inferior CAR-mediated effector function, and may have limited longevity, we aimed to increase the frequencies of T_{CM}- and T_{SCM}-derived cells during expansion of the cultures. We therefore compared the effects of the two cytokine regimens on relative T-cell subset expansion. To determine how IL-2 could influence the outgrowth of T_{CM} and T_{SCM} within bulk cultures, we reconstituted FACSort-purified T_{CM} and T_{SCM} as described earlier (Fig. 9A) followed by polyclonal activation with CD3 and CD28 antibodies in the presence of either IL-2 (50IU/mL) or IL-7 and IL-15 (each at 10ng/mL) and transduction with a retroviral vector encoding mOrange. We reconstituted each subset into its respective subset depleted population on day 3, then assessed the fate of T_{CM} and T_{SCM} by tracing their path in the course of expansion (Fig. 9B). The medium and cytokines were changed every 3 days during culture and expansion. The frequency and absolute numbers of each subset was assessed weekly for up to day 35 after the initial stimulation (Fig. 9C). Although the trend to higher frequencies of $CD4^+$ or $CD8^+$ T_{CM}- and T_{SCM}-derived cells induced by culture in IL-7 and IL-15 (Fig. 9C), did not reach significance, we plan to enhance this trend using cytokine modifications and to use our separation approach to validate the changes. Owing to the higher overall fold expansion rate of T-cells expanded in IL-7 and IL-15 the absolute numbers of T_{CM}- and T_{SCM}-derived cells were significantly higher than in IL-2-grown cultures (Fig. 9D). Furthermore, T-cells cultured in IL-2 showed an earlier contraction defined by reduction of cell numbers from day 20, whereas T-cells cultured in IL-7 and

IL-15 expanded long-term with no signs of culture contraction up to day 35 (Fig. 9D). These results confirm that IL-7 and IL-15 better supported the expansion of both T_{CM} and T_{SCM} within bulk cultures (24, 41).

Discussion

The central purpose of our study was to understand the contribution of naïve and effector/memory T-cell subsets to the bulk *in vitro*-stimulated CAR T-cell products that are eventually infused into patients on our clinical trials. To this end, we developed an approach to assess the fate of each T-cell subset by tracing its path in the course of expansion after transduction with either a GD2.CAR or a CD19.CAR and cultured alone or after reconstitution into the relevant subset-depleted PBMCs that had been activated and transduced in parallel (e.g. T_{SCM} into T_{SCM}-depleted PBMC). In our proof-of-concept study we show that all subsets were similarly susceptible to transduction, and the rate of T_{SUBSET} expansion was unchanged by transfer into the subset-depleted population. The greatest rate of expansion was observed in T_{SCM}-derived T-cells, but since T_{SCM} represented less than 1% (0.9±0.2%) of the starting population, their descendants comprised less than 2% of the final product on day 14. Naïve-derived T-cells showed the second greatest rate of expansion, and this population dominated the cultures by day 14, comprising up to 89% of CD19.CAR-modified T-cells. T_{CM} showed the 3rd greatest rate of proliferation and comprised up to 44% of the final population. T_{EM}- and T_{EMRA}-derived populations proliferated relatively poorly and were poorly represented in the final population (<5% and <3%, respectively). Despite the greatest proliferative response to TCR stimulation, the dominant naïve-derived T-cell majority showed relatively poor cytokine production, killing and poor proliferative responses to CAR stimulation. Further, T_{naive}-derived cells differentiated to a greater extent when cultured in the presence of memory T-cells compared to when cultured alone, and show reduced re-expansion capacity in response to CAR stimulation. IL-7 and IL-15 induced greater total fold expansion of CD3/28-activated T-cells and produced higher frequencies of T_{CM}– and T_{SCM}–derived cells than IL-2.

Successful CAR-T cell therapy depends on multiple cell and patient-dependent factors. Among these, the T-cell subset origin of the final T-cell product infused may be critical to the final outcome by contributing to post infusion T-cell expansion, effector function and long-term persistence (28, 36, 39). However, while the effector memory phenotype of the final CAR-T cell product infused is often described, the T-cell subset of origin is rarely investigated, so that functional dissection of the infusion product (T_{EFF} cell products) remains a prerequisite to better understand and correlate therapy outcome with T-cell product input. While individual subsets have been expanded in isolation, neither their expansion and function after reconstitution into the bulk population, nor the subset contribution to the final T-cell product have been reported. Of note, we analyzed the T-cell subset contribution only of PBMCs activated on CD3 and CD28-coated plates in the presence of either IL-7 and IL-15 or IL-2, which are the methods we have used to expand CAR-T-cells on our clinical trials. Many other methods are used by other groups, including CD3/28-coated beads, soluble CD3 and CD28 or PHA, and these may produce different results. Regardless, our strategy presents a means to evaluate the effects on T-cell subsets resulting from any changes in culture conditions.

There is intense discussion of the optimal phenotypic T-cell profile and optimal T-cell subset for immunotherapeutic use with regards to longevity, engraftment and anti-tumor effector function (24, 28, 30, 33, 36–39). Berger et al., showed that cytomegalovirus (CMV)-specific T_{EFF} clones derived from T_{CM} exhibited superior engraftment capacities compared to clones derived from T_{EM}, and were long-lived and established persistent memory T-cell in a primate model in which TCR stimulation was provided by endogenous CMV (32). Other groups have suggested that the naïve T-cell population is important since this subset may contain precursors for tumor-specific antigens that could contribute to tumor elimination (49). The question of whether naïve-derived T-cells displaying memory T-cell phenotypic characteristics have the capacity for long-term survival *in vivo*, particularly if they do not encounter their cognate antigen remains an important subject for investigation. Naïve to memory T-cell conversion is a very complex process that requires multiple encounters with antigen and occurs in secondary lymphoid organs that provide an environment for such conversion (50–53). Several studies reported effective *in vitro* T-cell priming for multiple viral and tumor antigens, however, their clinical efficacy remains to be demonstrated (54–62). In our studies, naïve-derived T-cells developed effector functions *in vitro*, but these were less potent than memory-derived T-cells. Whether such naïve-derived T-cells with a memory phenotype have long-term memory potential *in vivo* and whether *in vivo* CAR-stimulation by tumor cells can induce true memory conversion remains to be demonstrated.

Recently Sommermeyer et al. showed that when modified with a CD19.CAR, a combination of $CD4^+$ naïve- and $CD8^+$ T_{CM}-derived T-cells showed the most potent anti-tumor function *in vitro* and in preclinical models and in combination had synergistic anti-tumor effects in an EBV-positive lymphoma xenograft model (Raji) (63). This combination is currently under clinical evaluation. A possible advantage of the T_{CM} population is that it contains T-cells specific for endogenous viruses that may provide antigenic stimulation after infusion.

Gattinoni and colleagues described the existence of stem cell-like T-cells (T_{SCM}) within the phenotypically naïve ($CD45RA^+CCR7^+$) T-cell population (31). The expression of CD95 distinguished T_{SCM} ($CD45RA^+CCR7^+CD95^+$) from T_{naive} ($CD45RA^+CCR7^+CD95^-$), and in a murine xenograft model only T_{SCM} were able to serially transfer GVHD (41). The distinct functional and unique homeostatic properties of T_{SCM} have also been demonstrated in a nonhuman primate model during the course of simian immunodeficiency virus infection. In this report, T_{SCM} were described as the least-differentiated memory subset, functionally distinct from conventional memory cells and served as precursors of T_{CM} (40). In a human study, Xu and colleagues suggested that the frequency of T_{SCM}-like cells within the infused T-cell product correlated with *in vivo* expansion following adoptive transfer (38) while Biasco et al. showed that T_{SCM} produced the greatest contribution to long-term reconstitution in gene therapy studies using T-cells (64). Hence, T_{SCM} may have even greater potential for expansion and long-term persistence than T_{CM} (41), but to date, the relative benefits of T_{CM}- and T_{SCM}-derived CAR T-cells in clinical trials have not been reported. Our data suggest that standard strategies for CAR T-cell manufacturing may preferentially expand naïve T-cells with some contribution from T_{CM} but little contribution from T_{SCM}, despite the fact that they expand exponentially *in vitro* when cultured alone or within PBMC. Further studies are required to evaluate the long-term fate of T_{CM} and T_{SCM}-derived cells, both in culture and in patients.

The ultimate T-cell subset composition will likely also be affected by the CAR structure and endodomains, but our system provides a way to test these effects on the final infusion product. We show that culture conditions profoundly affect the subset composition of expanded T-cells. IL-2 expansion produced lower total fold expansion than IL-7 and IL-15 and thus decreased the numbers of T_{SCM} and T_{CM} in the final product. Although not significant, IL-7 and IL-15 also produced higher frequencies of T_{CM}– and T_{SCM}–derived cells than IL-2. Further efforts to improve the relative frequency of T_{CM}/ T_{SCM}-derived cells over naïve-derived T-cells could be validated using our strategy. Other culture manipulations including culture vessels, media formulation and type of initial stimulus will likely also influence the degree to which each subset contributes to the final population. Indeed in our prior study, we found that T_{SCM}-derived CMV-specific T-cells did not expand within the bulk population if they received stimulation with CMV peptides rather than CD3 and CD28 antibodies (24). A more direct way to obtain the desired T-cell subset is to separate it from the starting population prior to culture, but this increases the expense and complexity of manufacture (63). It would be instructive to know whether the manufacturing strategies used in various clinical trials promote the outgrowth of T_{CM} and T_{SCM} and useful to develop cell culture strategies that enhance their expansion within bulk cultures, without the requirement for separation strategies. We provide a strategy to evaluate the subsets of origin of T-cells grown under any conditions using PBMCs from patients or healthy donors. Our study supports the importance of IL-7 and IL-15 for the expansion of T_{CM} and T_{SCM}-derived effector T-cells, at least using our manufacturing strategy (38).

Although the different T-cell subsets were not differentially transduced by retroviral vectors, their dissimilar rates of proliferation led to changes in their relative frequencies in the final population, which was dominated by naïve-derived T-cells (76±19% of $CD3^+$ T-cells). T_{CM}-derived populations maintained their frequencies (30±12% of $CD3^+$ T-cells) and T_{SCM}-derived populations were maintained or slightly increased (mean of 1.5±0.3% of $CD3^+$ T-cells), while T_{EM} and T_{EMRA} frequencies were reduced (mean of 4.7±1.6% and 2.8±1.3% of $CD3^+$ T-cells, respectively). Although the majority of each subpopulation differentiated into cells with a T_{EM}-like phenotype, their functionalities differed with respect to cytokine production and proliferation in response to CAR stimulation. T_{naive}- and T_{EMRA}-derived cells produced lower levels of cytokines and proliferated poorly in response to CAR stimulation compared to T_{CM} and T_{SCM}-derived cells. This may be of little import for T_{EMRA}, since they comprise only a minor fraction of the final product, but a high frequency of poorly functional T_{naive}-derived cells may be less effective after infusion. Our results confirm reports suggesting that naïve-derived T-cells possess poor effector functions (39). However, we cannot exclude the possibility that naïve-derived T-cells will acquire improved function after multiple stimulations *in vivo* via the CAR, although they responded relatively poorly to a single CAR stimulation *in vitro*. Our data confirms the recent report by Klebanoff and colleagues showing enhanced phenotypic and functional differentiation of naïve-derived T-cells that have been cultured in the presence of antigen-experienced memory T-cell (29). Naïve-derived T-cells cultured in bulk PBMC preparations show reduced re-expansion capacity in response to CAR stimulation, and hence may lack anti-tumor potential when transferred *in vivo*. Nevertheless, when we cultured naïve-derived T-cells separately, re-expansion to CAR stimulation was reduced compared to T_{SCM}-, T_{CM}- and T_{EM}-derived

cultures. Hence, if naïve T-cells are to be used for adoptive immunotherapy, we would propose culture in isolation to avoid the negative effects of culture with antigen-experienced memory T-cells. Further *in vitro* and *in vivo* studies over longer time periods are required to determine the long-term consequences of infusing a preponderance of T_{naive}-derived cells, but without some form of differential gene-marking, this may be difficult.

Our strategy could also be used in cases in which short-lived effectors are desirable for safety reasons, for example to test a novel T-cell manipulation. Regardless, our strategy can be a powerful tool to evaluate the effects of manufacturing changes on the subset contribution to *in vitro* expanded T-cells. Certainly, a *one-size fit all strategy* for the generation of CAR-modified T_{EFF} may not be expected because of tumor cell biology and patient characteristics, but a better understanding of the characteristics of the generated CAR-modified T-cell products will help identify the subsets with most clinical efficacy. To this end, our strategy provides a powerful tool to elucidate the characteristics of CAR T-cells polyclonally expanded from PBMC on CD3 and CD28 antibody-coated plates, and to reveal the functional properties of each expanded T-cell subset.

Supplementary Material

Refer to Web version on PubMed Central for supplementary material.

Acknowledgments

We thank Dr. Jason Millward (Institute of Medical Immunology, Charité University Medicine Berlin and Experimental and Clinical Research Center, a joint cooperation between the Charité Medical Faculty and the Max-Delbrück Center for Molecular Medicine) for statistical advice. This project was supported in part by the Cytometry and Cell Sorting Core at Baylor College of Medicine and the expert assistance of Joel M. Sederstrom and team. We thank Dr. Juan F. Vera (Center for Gene Therapy, Baylor College of Medicine, Houston, TX, US) for the generous provision of the SFG.IRES.mOrange construct, Tatiana Goltsova and Dr. Amos Gaikwad (Texas Children's Hospital Flow Cytometry Core Laboratory) for technical flow cytometry assistance.

Funding: The study was generously supported in parts by the Deutsche Forschungsgemeinschaft (DFG-SFB-TR36-project A3), the German Federal Ministry of Education and Research (Berlin-Brandenburg Center for Regenerative Therapies grant), an Alex's Lemonade Stand Foundation grant to CMR, NIH-NCI PO1 CA94234 and P50 CA126752, the Cytometry and Cell Sorting Core at Baylor College of Medicine with funding from the NIH (P30 AI036211, P30 CA125123, and S10 RR024574) and The V-Foundation. The funders had no role in study design, data collection and analysis, decision to publish, or preparation of the manuscript.

Bibliography

1. Rosenberg, Sa, Restifo, NP., Yang, JC., Morgan, Ra, Dudley, ME. Adoptive cell transfer: a clinical path to effective cancer immunotherapy. Nat Rev Cancer. 2008; 8:299–308. [PubMed: 18354418]
2. Porter DL, Levine BL, Kalos M, Bagg A, June CH. Chimeric antigen receptor-modified T cells in chronic lymphoid leukemia. N Engl J Med. 2011; 365:725–33. [PubMed: 21830940]
3. Kalos M, Levine BL, Porter DL, Katz S, Grupp Sa, Bagg A, June CH. T cells with chimeric antigen receptors have potent antitumor effects and can establish memory in patients with advanced leukemia. Sci Transl Med. 2011; 3:95ra73.
4. Grupp, Sa, Kalos, M., Barrett, D., Aplenc, R., Porter, DL., Rheingold, SR., Teachey, DT., Chew, A., Hauck, B., Wright, JF., Milone, MC., Levine, BL., June, CH. Chimeric antigen receptor-modified T cells for acute lymphoid leukemia. N Engl J Med. 2013; 368:1509–18. [PubMed: 23527958]
5. Savoldo B, Ramos CA, Liu E, Mims MP, Keating MJ, Carrum G, Kamble RT, Bollard CM, Gee AP, Mei Z, Liu H, Grilley B, Rooney CM, Heslop HE, Brenner MK, Dotti G. Brief report CD28

costimulation improves expansion and persistence of chimeric antigen receptor – modified T cells in lymphoma patients. 2011; 121:1–5.

6. Kuwana Y, Asakura Y, Utsunomiya N, Nakanishi M, Arata Y, Itoh S, Nagase F, Kurosawa Y. Expression of chimeric receptor composed of immunoglobulin-derived V regions and T-cell receptor-derived C regions. Biochem Biophys Res Commun. 1987; 149:960–968. [PubMed: 3122749]
7. Gross G, Eshhar Z. Endowing T cells with antibody specificity using chimeric T cell receptors. FASEB J. 1992; 6:3370–8. [PubMed: 1464371]
8. Dotti G, Gottschalk S, Savoldo B, Brenner MK. Design and development of therapies using chimeric antigen receptor-expressing T cells. Immunol Rev. 2014; 257:107–26. [PubMed: 24329793]
9. Milone CM, Fish JD, Carpenito C, Carroll RG, Binder GK, Teachey D, Samanta M, Lakhal M, Gloss B, Danet-Desnoyers G, Campana D, Riley JL, Grupp Sa, June CH. Chimeric receptors containing CD137 signal transduction domains mediate enhanced survival of T cells and increased antileukemic efficacy in vivo. Mol Ther. 2009; 17:1453–1464. [PubMed: 19384291]
10. Zhong X, Matsushita M, Plotkin J, Riviere I, Sadelain M. Chimeric antigen receptors combining 4-1BB and CD28 signaling domains augment PI3kinase/AKT/Bcl-XL activation and CD8+ T cell-mediated tumor eradication. Mol Ther. 2010; 18:413–420. [PubMed: 19773745]
11. Savoldo B, Ramos CA, Liu E, Mims MP, Keating MJ, Carrum G, Kamble RT, Bollard CM, Gee AP, Mei Z, Liu H, Grilley B, Rooney CM, Heslop HE, Brenner MK, Dotti G. CD28 costimulation improves expansion and persistence of chimeric antigen receptor–modified T cells in lymphoma patients. J Clin Invest. 2011; 121:1822–1826. [PubMed: 21540550]
12. Till BG, Jensen MC, Wang J, Chen EY, Wood BL, Greisman Ha, Qian X, James SE, Raubitschek A, Forman SJ, Gopal AK, Pagel JM, Lindgren CG, Greenberg PD, Riddell SR, O. W. Press. Adoptive immunotherapy for indolent non-hodgkin lymphoma and mantle cell lymphoma using genetically modified autologous CD20-specific T cells. Blood. 2008; 112:2261–2271. [PubMed: 18509084]
13. Jensen MC, Popplewell L, Cooper LJ, DiGiusto D, Kalos M, Ostberg JR, Forman SJ. Antitransgene rejection responses contribute to attenuated persistence of adoptively transferred CD20/CD19-specific chimeric antigen receptor redirected T cells in humans. Biol Blood Marrow Transplant. 2010; 16:1245–56. [PubMed: 20304086]
14. Brentjens RJ, Rivière I, Park JH, Davila ML, Wang X, Stefanski J, Taylor C, Yeh R, Bartido S, Borquez-Ojeda O, Olszewska M, Bernal Y, Pegram H, Przybylowski M, Hollyman D, Usachenko Y, Pirraglia D, Hosey J, Santos E, Halton E, Maslak P, Scheinberg D, Jurcic J, Heaney M, Heller G, Frattini M, Sadelain M. Safety and persistence of adoptively transferred autologous CD19-targeted T cells in patients with relapsed or chemotherapy refractory B-cell leukemias. Blood. 2011; 118:4817–28. [PubMed: 21849486]
15. Kochenderfer JN, Wilson WH, Janik JE, Dudley ME, Stetler-Stevenson M, Feldman Sa, Maric I, Raffeld M, Nathan DAN, Lanier BJ, Morgan Ra, Rosenberg Sa. Eradication of B-lineage cells and regression of lymphoma in a patient treated with autologous T cells genetically engineered to recognize CD19. Blood. 2010; 116:4099–4102. [PubMed: 20668228]
16. Kochenderfer JN, Dudley ME, Carpenter RO, Kassim SH, Rose JJ, Telford WG, Hakim FT, Halverson DC, Fowler DH, Hardy NM, Mato AR, Hickstein DD, Gea-Banacloche JC, Pavletic SZ, Sportes C, Maric I, Feldman SA, Hansen BG, Wilder JS, Blacklock-Schuver B, Jena B, Bishop MR, Gress RE, Rosenberg Sa. Donor-derived CD19-targeted T cells cause regression of malignancy persisting after allogeneic hematopoietic stem cell transplantation. Blood. 2013; 122:4129–4139. [PubMed: 24055823]
17. Till BG, Jensen MC, Wang J, Qian X, Gopal AK, Maloney DG, Lindgren CG, Lin Y, Pagel JM, Budde LE, Raubitschek A, Forman SJ, Greenberg PD, Riddell SR, O. W. Press. CD20-specific adoptive immunotherapy for lymphoma using a chimeric antigen receptor with both CD28 and 4-1BB domains: Pilot clinical trial results. Blood. 2012; 119:3940–3950. [PubMed: 22308288]
18. Brentjens RJ, Davila ML, Riviere I, Park J, Wang X, Cowell LG, Bartido S, Stefanski J, Taylor C, Olszewska M, Borquez-Ojeda O, Qu J, Wasielewska T, He Q, Bernal Y, Rijo IV, Hedvat C, Kobos R, Curran K, Steinherz P, Jurcic J, Rosenblat T, Maslak P, Frattini M, Sadelain M. CD19-targeted

T cells rapidly induce molecular remissions in adults with chemotherapy-refractory acute lymphoblastic leukemia. Sci Transl Med. 2013; 5:177ra38.

19. Ritchie DS, Neeson PJ, Khot A, Peinert S, Tai T, Tainton K, Chen K, Shin M, Wall DM, Hönemann D, Gambell P, Westerman Da, Haurat J, Westwood Ja, Scott AM, Kravets L, Dickinson M, Trapani Ja, Smyth MJ, Darcy PK, Kershaw MH, Prince HM. Persistence and efficacy of second generation CAR T cell against the LeY antigen in acute myeloid leukemia. Mol Ther. 2013; 21:2122–9. [PubMed: 23831595]
20. Cruz CRY, Micklethwaite KP, Savoldo B, Ramos CA, Lam S, Ku S, Diouf O, Liu E, Barrett AJ, Ito S, Shpall EJ, Krance RA, Kamble RT, Carrum G, Hosing CM, Gee AP, Mei Z, Grilley BJ, Heslop HE, Rooney CM, Brenner MK, Bollard CM, Dotti G. Infusion of donor-derived CD19-redirected virus-specific T cells for B-cell malignancies relapsed after allogeneic stem cell transplant: a phase 1 study. Blood. 2013; 122:2965–73. [PubMed: 24030379]
21. Maus MV, Grupp Sa, Porter DL, June CH. Antibody-modified T cells: CARs take the front seat for hematologic malignancies. Blood. 2014; 123:2625–35. [PubMed: 24578504]
22. Dotti G, Gottschalk S, Savoldo B, Brenner MK. Design and development of therapies using chimeric antigen receptor-expressing T cells. Immunol Rev. 2014; 257:107–26. [PubMed: 24329793]
23. Hudecek M, Lupo-Stanghellini MT, Kosasih PL, Sommermeyer D, Jensen MC, Rader C, Riddell SR. Receptor affinity and extracellular domain modifications affect tumor recognition by ROR1-specific chimeric antigen receptor T cells. Clin Cancer Res. 2013; 19:3153–3164. [PubMed: 23620405]
24. Schmueck-Henneresse M, Sharaf R, Vogt K, Weist BJD, Landwehr-Kenzel S, Fuehrer H, Jurisch A, Babel N, Rooney CM, Reinke P, Volk H-D. Peripheral Blood-Derived Virus-Specific Memory Stem T Cells Mature to Functional Effector Memory Subsets with Self-Renewal Potency. J Immunol. 2015
25. Savoldo B, Goss Ja, Hammer MM, Zhang L, Lopez T, Gee AP, Lin Y-F, Quiros-Tejeira RE, Reinke P, Schubert S, Gottschalk S, Finegold MJ, Brenner MK, Rooney CM, Heslop HE. transplant recipients with autologous Epstein Barr virus-specific cytotoxic T lymphocytes (CTLs). Blood. 2006; 108:2942–9. [PubMed: 16835376]
26. Bollard CM, Rooney CM, Heslop HE. T-cell therapy in the treatment of post-transplant lymphoproliferative disease. Nat Rev Clin Oncol. 2012; 9:510–9. [PubMed: 22801669]
27. Brestrich G, Zwinger S, Fischer A, Schmück M, Röhmhild A, Hammer MH, Kurtz A, Uharek L, Knosalla C, Lehmkuhl H, Volk H-D, Reinke P. Adoptive T-cell therapy of a lung transplanted patient with severe CMV disease and resistance to antiviral therapy. Am J Transplant. 2009; 9:1679–84. [PubMed: 19459791]
28. Terakura S, Yamamoto TN, Gardner Ra, Turtle CJ, Jensen MC, Riddell SR. Generation of CD19-chimeric antigen receptor modified CD8+ T cells derived from virus-specific central memory T cells. Blood. 2012; 119:72–82. [PubMed: 22031866]
29. Klebanoff CA, Scott CD, Leonardi AJ, Yamamoto TN, Cruz AC, Ouyang C, Ramaswamy M, Roychoudhuri R, Ji Y, Eil RL, Sukumar M, Crompton JG, Palmer DC, Borman ZA, Clever D, Thomas SK, Patel S, Yu Z, Muranski P, Liu H, Wang E, Marincola FM, Gros A, Gattinoni L, Rosenberg SA, Siegel RM, Restifo NP. Memory T cell-driven differentiation of naive cells impairs adoptive immunotherapy. J Clin Invest. 2016; 126:318–334. [PubMed: 26657860]
30. Sallusto F, Lenig D, Förster R, Lipp M, Lanzavecchia A. Two subsets of memory T lymphocytes with distinct homing potentials and effector functions. Nature. 1999; 401:708–712. [PubMed: 10537110]
31. Gattinoni L, Lugli E, Ji Y, Pos Z, Paulos CM, Quigley MF, Almeida JR, Gostick E, Yu Z, Carpenito C, Wang E, Douek DC, Price DA, June CH, Marincola FM, Roederer M, Restifo NP. A human memory T cell subset with stem cell-like properties. Nat Med. 2011; 17:1290–1297. [PubMed: 21926977]
32. Berger C, Jensen MC, Lansdorp PM, Gough M, Elliott C, Riddell SR. Adoptive transfer of effector CD8+ T cells derived from central memory cells establishes persistent T cell memory in primates. J Clin Invest. 2008; 118:294–305. [PubMed: 18060041]
33. Schmueck M, Fischer AM, Hammoud B, Brestrich G, Fuehrer H, Luu S-H, Mueller K, Babel N, Volk H-D, Reinke P. Preferential expansion of human virus-specific multifunctional central

memory T cells by partial targeting of the IL-2 receptor signaling pathway: the key role of CD4+ T cells. J Immunol. 2012; 188:5189–98. [PubMed: 22516956]

34. Carrasco J, Godelaine D, Van Pel A, Boon T, Van Der Bruggen P. CD45RA on human CD8 T cells is sensitive to the time elapsed since the last antigenic stimulation. Blood. 2006; 108:2897–2905. [PubMed: 16857986]
35. Wang X, Berger C, Wong CW, Forman SJ, Riddell SR, Jensen MC. Engraftment of human central memory-derived effector CD8+ T cells in immunodeficient mice. Blood. 2011; 117:1888–98. [PubMed: 21123821]
36. Wang X, Naranjo A, Brown CE, Bautista C, Wong CW, Chang W-C, Aguilar B, Ostberg JR, Riddell SR, Forman SJ, Jensen MC. Phenotypic and functional attributes of lentivirus-modified CD19-specific human CD8+ central memory T cells manufactured at clinical scale. J Immunother. 2012; 35:689–701. [PubMed: 23090078]
37. Riddell SR, Sommermeyer D, Berger C, Liu LS, Balakrishnan A, Salter A, Hudecek M, Maloney DG, Turtle CJ. Adoptive therapy with chimeric antigen receptor-modified T cells of defined subset composition. Cancer J. 2014; 20:141–4. [PubMed: 24667960]
38. Xu Y, Zhang M, Ramos Ca, Durett A, Liu E, Dakhova O, Liu H, Creighton CJ, Gee AP, Heslop HE, Rooney CM, Savoldo B, Dotti G. Closely related T-memory stem cells correlate with in vivo expansion of CAR.CD19-T cells and are preserved by IL-7 and IL-15. Blood. 2014; 123:3750–9. [PubMed: 24782509]
39. Hinrichs CS, Borman Za, Gattinoni L, Yu Z, Burns WR, Huang J, Klebanoff Ca, Johnson La, Kerkar SP, Yang S, Muranski P, Palmer DC, Scott CD, Morgan Ra, Robbins PF, Rosenberg Sa, Restifo NP. Human effector CD8+ T cells derived from naive rather than memory subsets possess superior traits for adoptive immunotherapy. Blood. 2011; 117:808–814. [PubMed: 20971955]
40. Lugli E, Dominguez MH, Gattinoni L, Chattopadhyay PK, Bolton DL, Song K, Klatt NR, Brenchley JM, Vaccari M, Gostick E, Price Da, Waldmann Ta, Restifo NP, Franchini G, Roederer M. Superior T memory stem cell persistence supports long-lived T cell memory. J Clin Invest. 2013; 123:594–9. [PubMed: 23281401]
41. Cieri N, Camisa B, Cocchiarella F, Forcato M, Oliveira G, Provasi E, Bondanza A, Bordignon C, Peccatori J, Ciceri F, Lupo-Stanghellini MT, Mavilio F, Mondino A, Bicciato S, Recchia A, Bonini C. IL-7 and IL-15 instruct the generation of human memory stem T cells from naive precursors. Blood. 2013; 121:573–84. [PubMed: 23160470]
42. Lugli E, Gattinoni L, Roberto A, Mavilio D, Price Da, Restifo NP, Roederer M. Identification, isolation and in vitro expansion of human and nonhuman primate T stem cell memory cells. Nat Protoc. 2013; 8:33–42. [PubMed: 23222456]
43. Pulè, Ma, Straathof, KC., Dotti, G., Heslop, HE., Rooney, CM., Brenner, MK. A chimeric T cell antigen receptor that augments cytokine release and supports clonal expansion of primary human T cells. Mol Ther. 2005; 12:933–41. [PubMed: 15979412]
44. Rossig C, Bollard CM, Nuchtern JG, Merchant DA, Brenner MK. Targeting of GD2-positive tumor cells by human T lymphocytes engineered to express chimeric T-cell receptor genes. Int J Cancer. 2001; 94:228–236. [PubMed: 11668503]
45. Loskog A, Giandomenico V, Rossig C, Pule M, Dotti G, Brenner MK. Addition of the CD28 signaling domain to chimeric T-cell receptors enhances chimeric T-cell resistance to T regulatory cells. Leukemia. 2006; 20:1819–28. [PubMed: 16932339]
46. Sen G, Chakraborty M, Foon KA, Reisfeld RA, Bhattacharya-Chatterjee M. Preclinical evaluation in nonhuman primates of murine monoclonal anti- idiotype antibody that mimics the disialoganglioside GD2. Clin Cancer Res. 1997; 3:1969–1976. [PubMed: 9815586]
47. Hermans IF, Silk JD, Yang J, Palmowski MJ, Gileadi U, McCarthy C, Salio M, Ronchese F, Cerundolo V. The VITAL assay: A versatile fluorometric technique for assessing CTL- and NKT-mediated cytotoxicity against multiple targets in vitro and in vivo. J Immunol Methods. 2004; 285:25–40. [PubMed: 14871532]
48. Hammoud B, Schmueck M, Fischer AM, Fuehrer H, Park S-J, Akyuez L, Schefold JC, Raftery MJ, Schönrich G, Kaufmann AM, Volk H-D, Reinke P. HCMV-specific T-cell therapy: do not forget supply of help. J Immunother. 2013; 36:93–101. [PubMed: 23377662]

49. Wölfl M, Merker K, Morbach H, Van Gool SW, Eyrich M, Greenberg PD, Schlegel PG. Primed tumor-reactive multifunctional CD62L+ human CD8 + T cells for immunotherapy. Cancer Immunol Immunother. 2011; 60:173–186. [PubMed: 20972785]
50. Grakoui A. The Immunological Synapse: A Molecular Machine Controlling T Cell Activation. Science (80-). 1999; 285:221–227.
51. Bousso P, Robey E. Dynamics of CD8+ T cell priming by dendritic cells in intact lymph nodes. Nat Immunol. 2003; 4:579–585. [PubMed: 12730692]
52. Stoll S, Delon J, Brotz TM, Germain RN. Dynamic imaging of T cell-dendritic cell interactions in lymph nodes. Science. 2002; 296:1873–6. [PubMed: 12052961]
53. Mempel TR, Henrickson SE, Von Andrian UH. T-cell priming by dendritic cells in lymph nodes occurs in three distinct phases. Nature. 2004; 427:154–9. [PubMed: 14712275]
54. Berard F, Blanco P, Davoust J, Neidhart-Berard EM, Nouri-Shirazi M, Taquet N, Rimoldi D, Cerottini JC, Banchereau J, Palucka AK. Cross-priming of naive CD8 T cells against melanoma antigens using dendritic cells loaded with killed allogeneic melanoma cells. J Exp Med. 2000; 192:1535–44. [PubMed: 11104796]
55. Moser JM, Sassano ER, Leistritz DC, Eatrides JM, Phogat S, Koff W, Drake DR. Optimization of a dendritic cell-based assay for the in vitro priming of naïve human CD4+ T cells. J Immunol Methods. 2010; 353:8–19. [PubMed: 19925804]
56. Hanley PJ, Melenhorst JJ, Nikiforow S, Scheinberg P, Blaney JW, Demmler-Harrison G, Cruz CR, Lam S, Krance RA, Leung KS, Martinez CA, Liu H, Douek DC, Heslop HE, Rooney CM, Shpall EJ, Barrett AJ, Rodgers JR, Bollard CM. CMV-specific T cells generated from naïve T cells recognize atypical epitopes and may be protective in vivo. Sci Transl Med. 2015; 7:285ra63.
57. Ho WY, Nguyen HN, Wolfl M, Kuball J, Greenberg PD. In vitro methods for generating CD8+ T-cell clones for immunotherapy from the naive repertoire. J Immunol Methods. 2006; 310:40–52. [PubMed: 16469329]
58. Wölfl M, Greenberg PD. Antigen-specific activation and cytokine-facilitated expansion of naive, human CD8+ T cells. Nat Protoc. 2014; 9:950–66. [PubMed: 24675735]
59. Schlienger K, Craighead N, Lee KP, Levine BL, June CH. Efficient priming of protein antigen-specific human CD4(+) T cells by monocyte-derived dendritic cells. Blood. 2000; 96:3490–3498. [PubMed: 11071646]
60. Santegoets SJAM, Schreurs MWJ, Masterson AJ, Liu YP, Goletz S, Baumeister H, Kueter EWM, Lougheed SM, Van Den Eertwegh AJM, Scheper RJ, Hooijberg E, De Gruijl TD. In vitro priming of tumor-specific cytotoxic T lymphocytes using allogeneic dendritic cells derived from the human MUTZ-3 cell line. Cancer Immunol Immunother. 2006; 55:1480–1490. [PubMed: 16468034]
61. Nguyen HH, Kim T, Song SY, Park S, Cho HH, Jung S-H, Ahn J-S, Kim H-J, Lee J-J, Kim H-O, Cho J-H, Yang D-H. Naïve CD8(+) T cell derived tumor-specific cytotoxic effectors as a potential remedy for overcoming TGF-β immunosuppression in the tumor microenvironment. Sci Rep. 2016; 6:28208. [PubMed: 27306834]
62. Tuettenberg A, Jonuleit H, Tüting T, Brück J, Knop J, Enk AH. Priming of T cells with Ad-transduced DC followed by expansion with peptide-pulsed DC significantly enhances the induction of tumor-specific CD8+ T cells: implications for an efficient vaccination strategy. Gene Ther. 2003; 10:243–50. [PubMed: 12571632]
63. Sommermeyer D, Hudecek M, Kosasih PL, Gogishvili T, Maloney DG, Turtle CJ, Riddell SR. Chimeric antigen receptor-modified T cells derived from defined CD8+ and CD4+ subsets confer superior antitumor reactivity in vivo. Leukemia. 2015:1–9.
64. Biasco L, Scala S, Basso Ricci L, Dionisio F, Baricordi C, Calabria A, Giannelli S, Cieri N, Barzaghi F, Pajno R, Al-Mousa H, Scarselli A, Cancrini C, Bordignon C, Roncarolo MG, Montini E, Bonini C, Aiuti A. In vivo tracking of T cells in humans unveils decade-long survival and activity of genetically modified T memory stem cells. Sci Transl Med. 2015; 7:273ra13–273ra13.

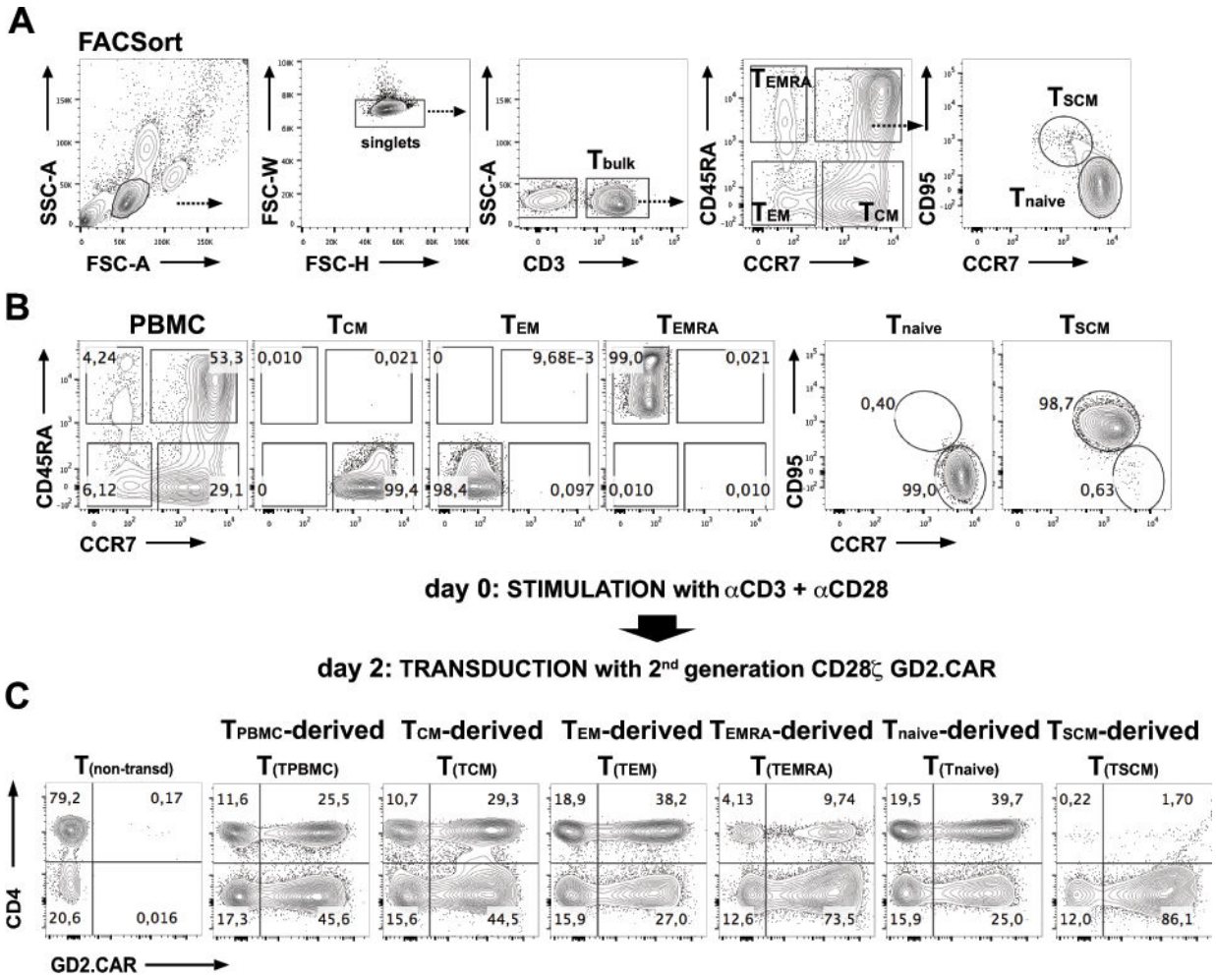

FIGURE 1. Strategy for T-cell subset sorting, activation and transduction

(A) Illustrates the strategy for sorting T-cell subsets from PBMC according to their expression of $CD3^+$, $CD45RA^+$, $CCR7^+$ and $CD95^+$. Prior to FACSorting, $CD3^+$ T-cells were enriched from PBMC by untouched MACS separation. They were then sorted into the following subsets: T_{CM} ($CCR7^+CD45RA^-$), T_{EM} ($CCR7^-CD45RA^-$), T_{EMRA} ($CCR7^-CD45RA^+$), T_{SCM} ($CD45RA^+CCR7^+ \rightarrow CD95^+$) and T_{naive} ($CD45RA^+CCR7^+ \rightarrow CD95^-$). (**B**) FACSort purified T-cell populations were isolated to greater than 98% purity. (**C**) Strategy for polyclonal activation and retroviral transduction of PBMC-derived $T_{(TPBMC)}$, T_{CM}-derived ($T_{(TCM)}$), T_{EM}-derived ($T_{(TEM)}$), T_{EMRA}-derived ($T_{(TEMRA)}$), T_{SCM}-derived ($T_{(TSCM)}$) and T_{naive}-derived ($T_{(Tnaive)}$) cells. FACSort purified T_{SUBSET} were activated with CD3 and CD28 antibodies and cultured in the presence of IL-7 and IL-15 at 10ng/mL each and transduced on day 2 with a 2nd generation GD2.CAR (14g2a.CD28-ζ CAR). Shown are examples of GD2.CAR transduction efficacies in separately cultured PBMC-, T_{CM}-, T_{EM}-, T_{EMRA}-, T_{SCM}- and T_{naive}-derived populations on day 7 post activation. Transduction efficacies were assessed by fluorescence staining for the GD2.CAR expression on the T-cell surface using the 1A7 antibody targeting 14g2a.

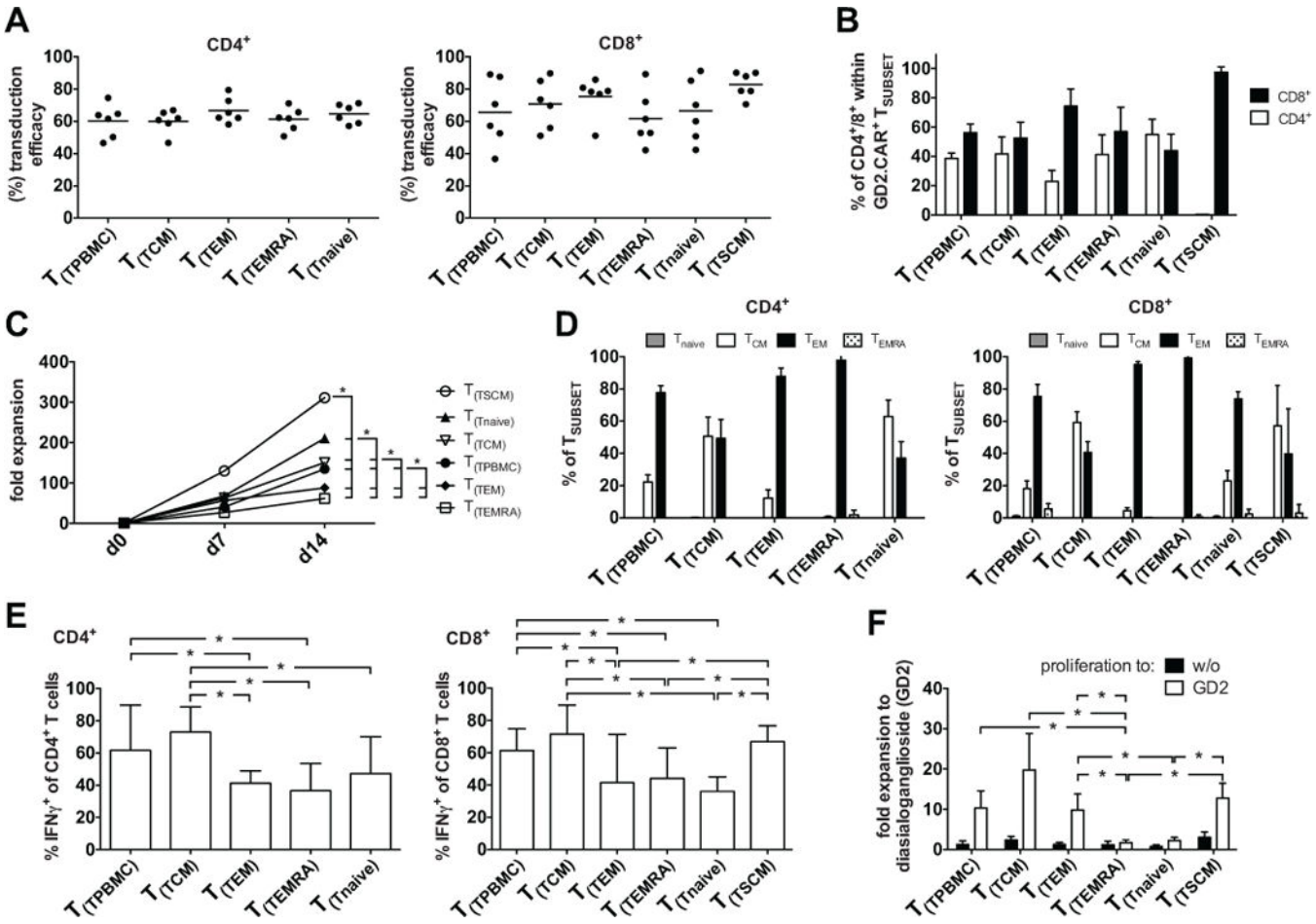

FIGURE 2. Fold Expansion and phenotype of separately cultured GD2.CAR-modified $T_{SUBSETS}$ in response to GD2 stimulation

(**A**) FACSort purified T_{SUBSET} were cultured according to Fig. 1. GD2 transduction efficacies from 6 donors: left graph: $CD4^+$; right graph: $CD8^+$ T_{SUBSET}-derived ($T_{(TSUBSET)}$) populations on day 14 after CD3/28-activation. (**B**) $CD4^+/CD8^+$ proportion within GD2.CAR^+ $T_{SUBSETS}$. (**C**) T_{SUBSET} expansion in response to CD3/28 stimulation (measured as fold increase) analyzed for each T_{SUBSET} on days 7 and 14. (**D**) Quantification of CCR7 and CD45RO expression 14 days after CD3/28-activation in each T_{SUBSET}-derived population: T_{CM} ($CCR7^+CD45RO^+$), T_{EM} ($CCR7^-CD45RO^+$), T_{EMRA} ($CCR7^-CD45RO^-$) and T_{naive} ($CCR7^+CD45RO^-$). Left graph: $CD4^+$; right graph: $CD8^+$ T_{SUBSET}-derived populations. (**E**) CD3/28-expanded T_{SUBSET}-derived populations were re-stimulated via the CAR using a GD2-positive neuroblastoma cell line, JF at a stimulator to responder ratio of 10:1 14 days after the initial CD3/28 activation and a non-CAR control stimulation ($GD2^-$ Hodgkin lymphoma: HDLM-2). Shown is background-subtracted (negative control: HDLM-2) IFN**γ** production to JF by $CD4^+$ (left graph) and $CD8^+$ (right graph) T_{SUBSET}-derived populations and was determined by intracellular staining 6 hrs after co-culture. Cells were permeabilized and stained for IFN**γ**, CD3, CD4 and CD8. (**F**) T_{SUBSET} expansion (measured as fold increase) was analyzed for each cell subset between days 14 and 21 after stimulation with plate-bound GD2 on day 14. Mean data from 6 healthy donors are

presented, and error bars represent SEM. Data were analyzed using repeated measures 1-way ANOVA, after verifying Gaussian distribution with the Kolmogorov-Smirnov test. p-values ≤ 0.05 were considered significant: *p<0.05.

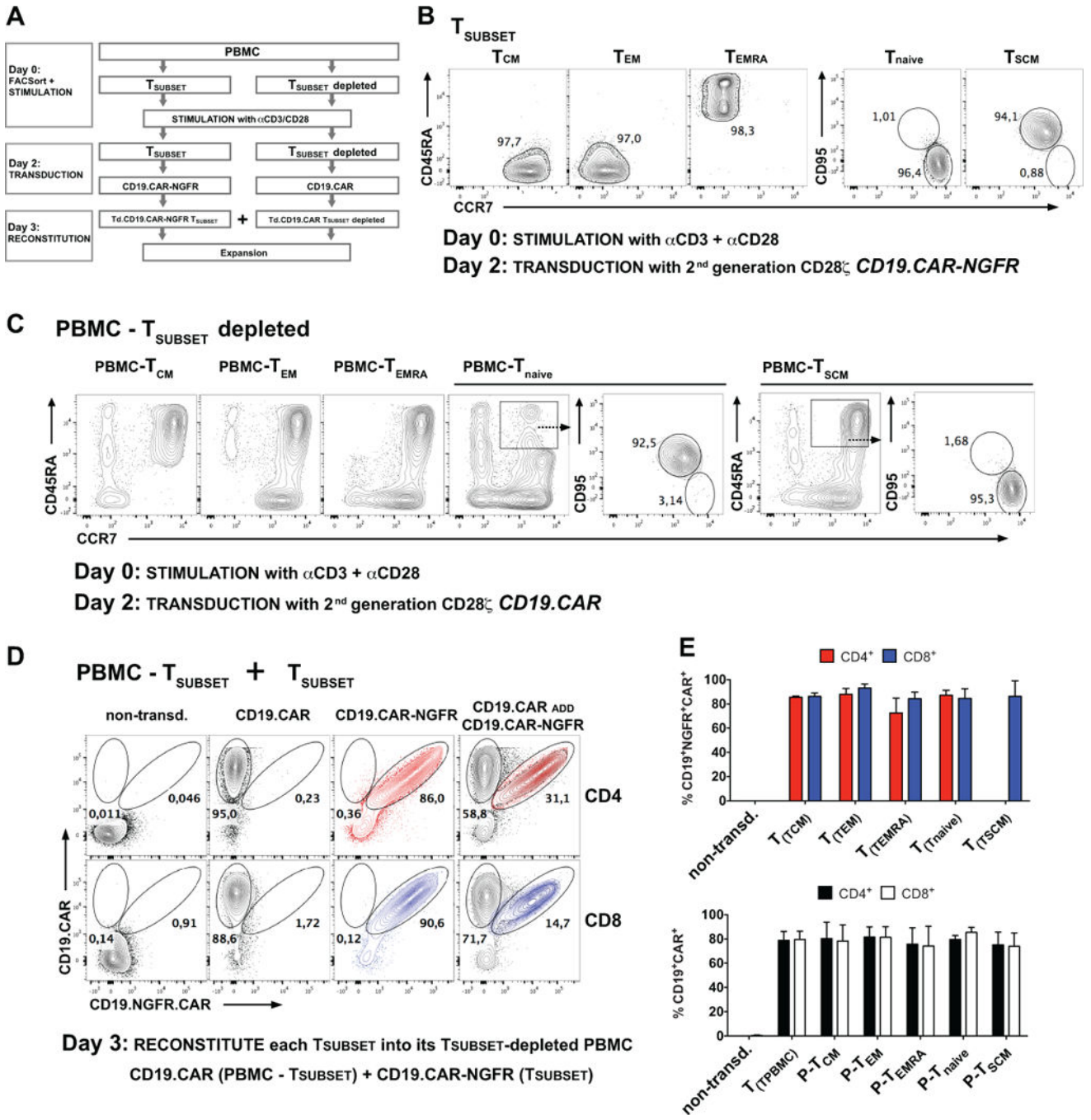

FIGURE 3. Experimental design to assess the fate of $T_{SUBSETS}$ polyclonally expanded within PBMC

(**A**) Illustrates the strategy for FACSort-purification of T-cell populations: T_{CM}, T_{EM}, T_{EMRA}, T_{naive} and T_{SCM} were FACSort-depleted from PBMC (**B**: $T_{SUBSETS}$; **C**: PBMC-T_{CM}, PBMC-T_{EM}, PBMC-T_{EMRA}, PBMC-T_{naive}, PBMC-T_{SCM}). After isolation each T_{SUBSET} and each single subset-depleted PBMC population was activated with CD3 and CD28 antibodies in the presence of IL-7 and IL-15, then transduced on day 2 with a CD19.CAR construct encoding a marker gene (NGFR), while T_{SUBSET}–depleted cells were

transduced with the CD19.CAR alone (CD19.CD28ζ CAR). Each activated and transduced T_{SUBSET} was reconstituted into the appropriate activated and transduced T_{SUBSET} –depleted PBMC at their initial frequencies one day after transduction to allow tracking of the subset within the bulk population after reconstitution (details in methods). (**D**) Representative FACS plots are shown for the flow cytometric detection of each reconstituted CD19.CAR-$NGFR^+$ T_{SUBSET}-derived ($T_{(TSUBSET)}$) population ($CD4^+$ $T_{(TSUBSET)}$ indicated in red dots; $CD8^+$ $T_{(TSUBSET)}$ indicated in blue dots) and $CD19.CAR^+$ PBMC-T_{SUBSET} (P-$T_{SUBSET,}$ gray dots) by the assessment of the CD19.CAR and the CD19.CAR-$NGFR^+$, respectively. (**E**; upper graph) CD19.CAR-NGFR transduction efficacies for $CD4^+$ and $CD8^+$ T_{CM}, T_{EM}, T_{EMRA}, T_{SCM} and T_{naive}-derived ($T_{(TSUBSET)}$) population and (**E**; lower graph) CD19.CAR transduction efficacies for $CD4^+$ and $CD8^+$ PBMC-T_{SUBSET} (P-T_{SUBSET}).

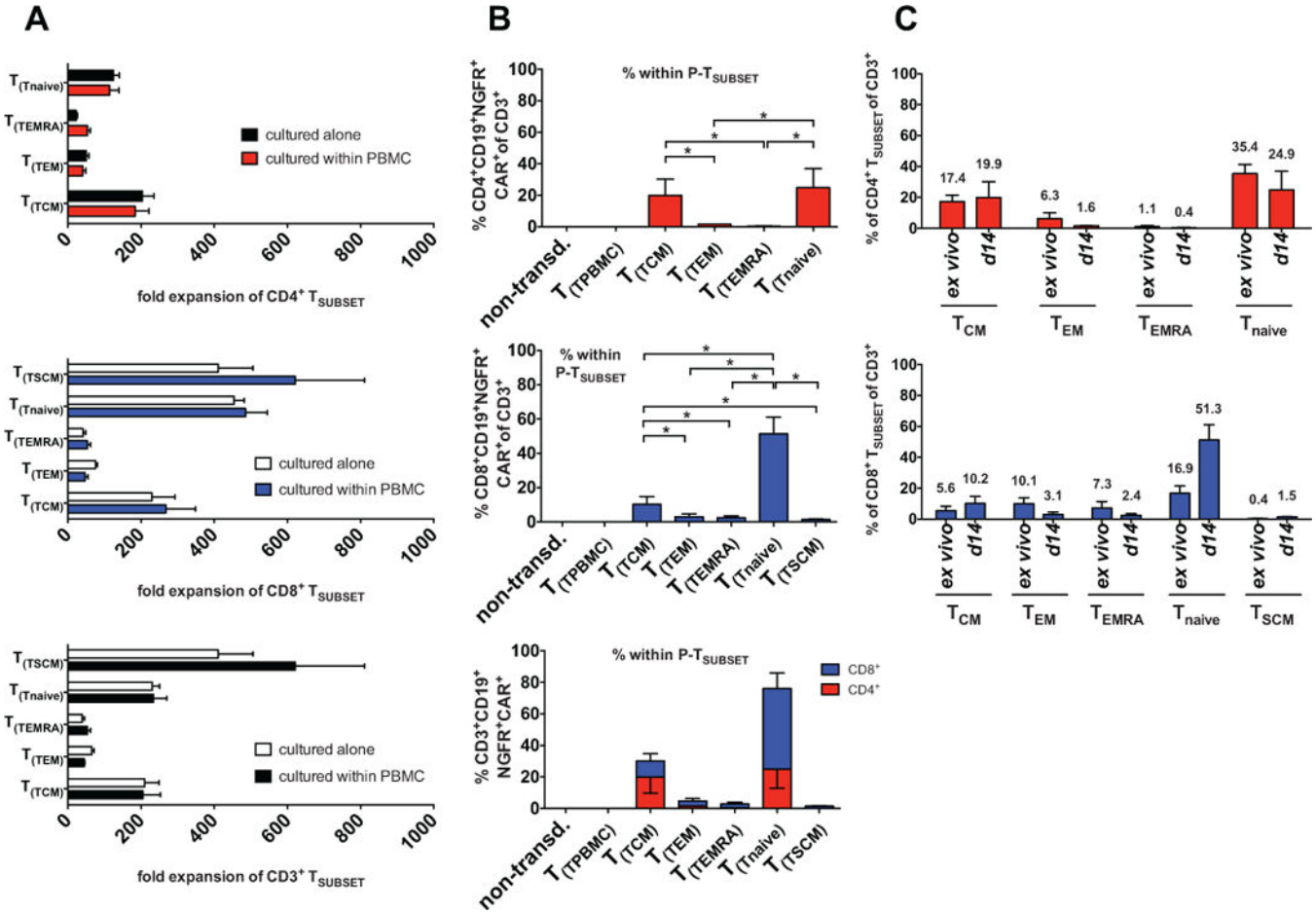

FIGURE 4. Fate of $T_{SUBSETS}$ polyclonally expanded within PBMC: naïve-derived T-cells expand preferentially within polyclonally activated PBMC

CAR-modified T_{SUBSET} were reconstituted into CD19.CAR modified, subset-depleted PBMC according to Figure 3. (**A**) Fold expansion of CD19.CAR-NGFR$^+$ T_{SUBSET}-derived ($T_{(TSUBSET)}$) population cultured alone or after reconstitution into the PBMC-T_{SUBSET}: CD4$^+$ (upper graph), CD8$^+$ (middle graph) and whole CD3$^+$ (lower graph). (**B**) Analysis on day 14 post initial polyclonal activation of each $T_{(TSUBSET)}$ (CD19.CAR-NGFR$^+$) within PBMC-T_{SUBSET} expanded T-cells (CD19.CAR$^+$) showing higher frequencies of CD4$^+$ (red, upper graph), CD8$^+$ (blue, middle graph) and whole CD3$^+$ (lower graph) $T_{(Tnaive)}$ and $T_{(TCM)}$ cells compared to other $T_{(TSUBSET)}$. Data were analyzed using repeated measures 1-way ANOVA, after verifying Gaussian distribution with the Kolmogorov-Smirnov test. p-values ≤ 0.05 were considered significant: *p<0.05. (**C**) Frequency of each T_{SUBSET} within CD3$^+$ PBMC (*ex vivo*) and frequency at day 14 of CD4$^+$ (red, upper graph) and CD8$^+$ (blue, lower graph) CD19.CAR-NGFR$^+$ $T_{(TSUBSET)}$ within PBMC-T_{SUBSET} expanded T-cells. Mean data from 6 healthy donors are presented, and error bars represent SEM.

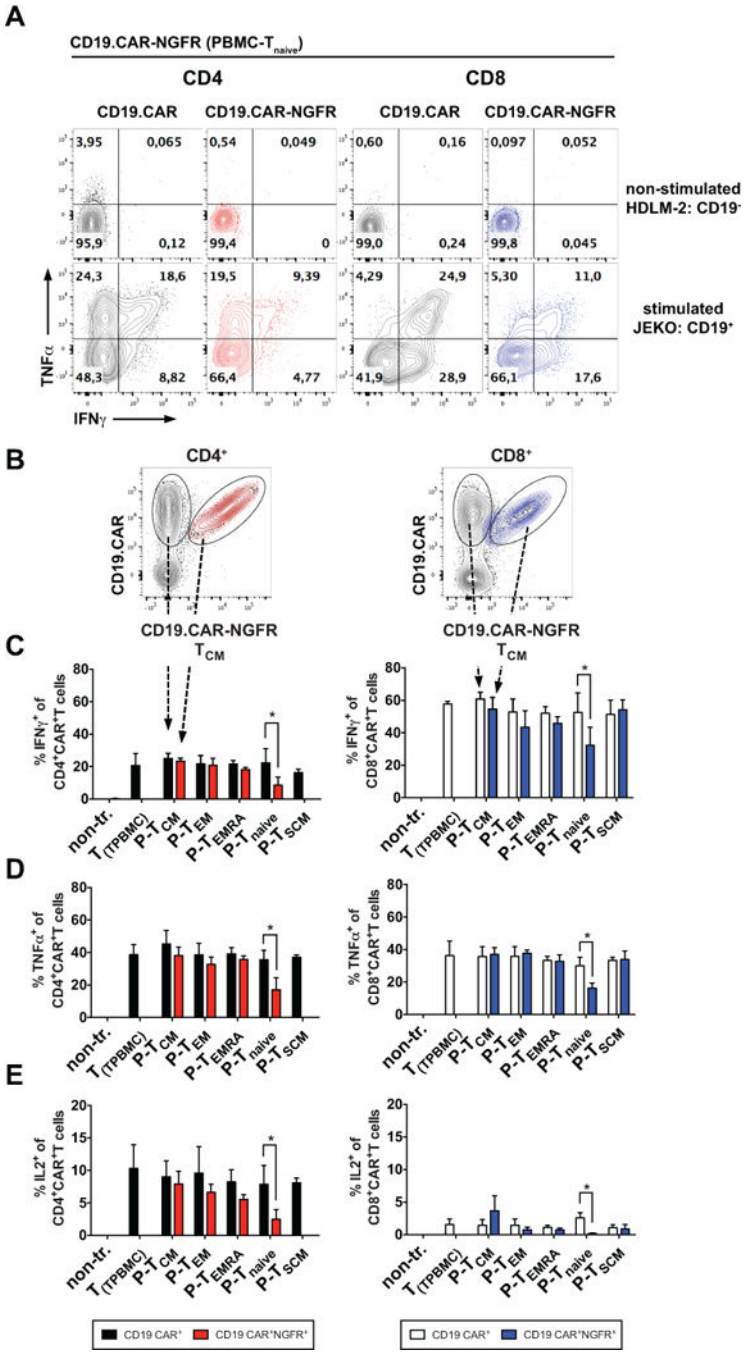

FIGURE 5. Cytokine production by reconstituted T-cell subsets in response to CAR-stimulation

CAR-modified T-cell subsets were reconstituted into CD19.CAR modified, subset-depleted PBMC according to Figure 3. On day 14, cultures were stimulated with a $CD19^{-}$ (HDLM-2) or $CD19^{+}$ JEKO lymphoma cells for 6 hrs at a stimulator to responder ratio of 10:1. Cytokine production was measured by intracellular cytokine staining. (**A**) Shows a representative FACSplot in which IFNγ and TNFα production by T_{naive}–derived cells in response to HDLM-2 (upper plots) or JEKO (lower plots) is shown. $T_{SUBSETS}$ could be distinguished from the depleted fraction by their expression of NGFR (**B**). The fraction of all

subsets producing IFNγ, TNFα, IL-2 is shown for $CD4^+$ and $CD8^+$ T-cells in **C**, **D** and **E**. Cytokine production by transduced and non-transduced PBMC is also shown. Black bars represent PBMC-T_{SUBSET}–derived $CD4^+$ T-cells, red bars represent T_{SUBSET}–derived $CD4^+$ T-cells, white bars represent PBMC-T_{SUBSET}–derived $CD8^+$ T-cells, blue bars represent T_{SUBSET}–derived $CD8^+$ T-cells. Data from T_{SUBSET}–derived (CD19.CAR-$NGFR^+$) and PBMC-T_{SUBSET}–derived (CD19.CAR^+) populations within one approach were analyzed using paired t-test, after verifying Gaussian distribution with the Kolmogorov-Smirnov test. p-values ≤ 0.05 were considered significant: *$p<0.05$. Mean data from 3 healthy donors are presented, and error bars represent SEM.

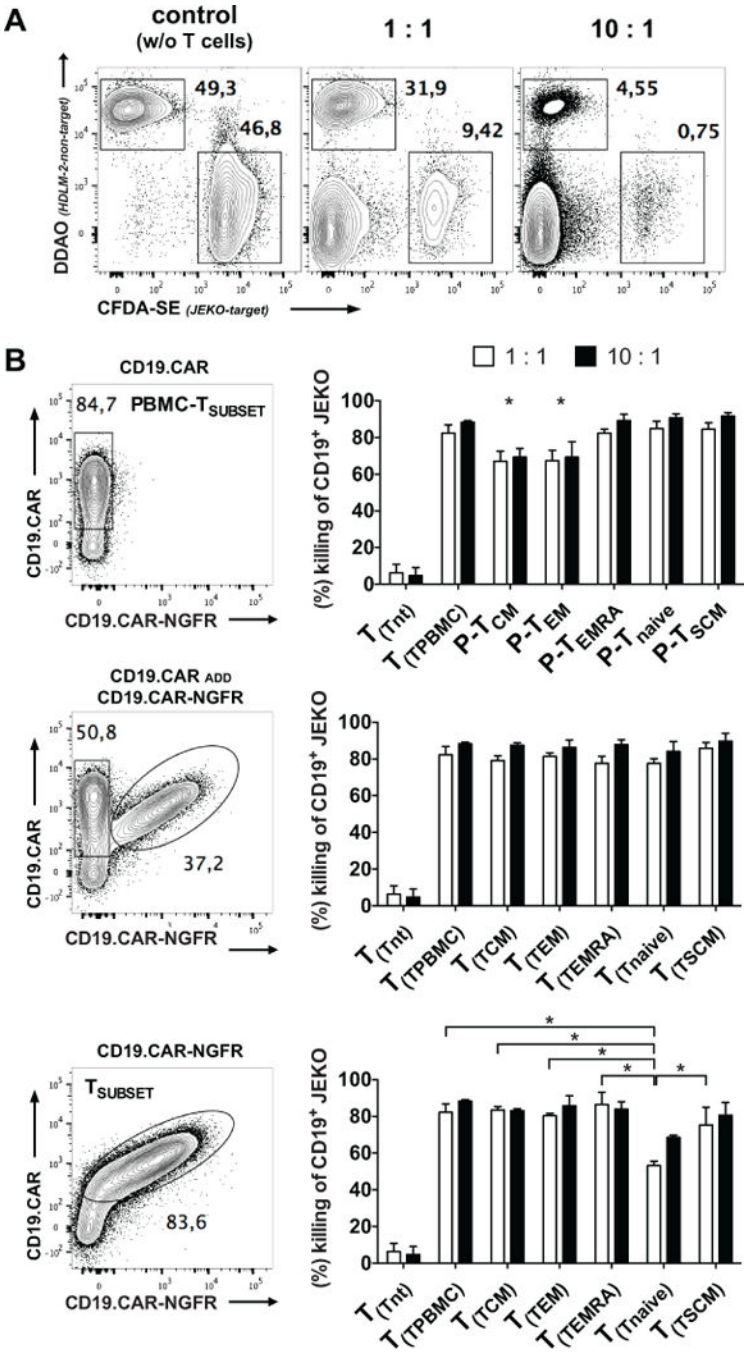

FIGURE 6. Cytotoxic killing capacity of each T_{SUBSET}–derived population cultured alone and its respective T_{SUBSET}-depleted and T_{SUBSET}-reconstituted PBMC cell preparation

Assessment of cytotoxic activity by flow cytometric *vital assay*. CAR-modified T-cell subsets were cultured alone or reconstituted into CD19.CAR modified, subset-depleted PBMC according to Figure 3. (**A**) CFDA-SE$^+$ CD19$^+$ JEKO cell lines (serving as stimulator APC for 2nd generation CD19.CAR T-cells) were used as targets, whereas DDOA$^+$ CD19$^-$ HDLM-2 cells lack CD19 were used as control targets. Cells were co-cultured for 16 hrs in T-cell / target cell ratio of 1:1 and 10:1. Samples without T-cells, containing only APC (CD19$^+$ JEKO cell lines or CD19$^-$ HDLM-2) displayed as internal control. The mean

percent survival of $CD19^+$ JEKO incubated targets was calculated relative to $CD19^-$ HDLM-2 controls. (**B**) Shows the killing capacity of each T_{SUBSET}-depleted bulk population (upper panel), T_{SUBSET}-reconstituted bulk population (middle panel) and T_{SUBSET} cultured alone (lower panel). Data from T_{SUBSET}–derived population cultured alone, T_{SUBSET}-depleted and T_{SUBSET}-reconstituted PBMC cell preparations were analyzed using paired t-test, after verifying Gaussian distribution with the Kolmogorov-Smirnov test. p-values ≤ 0.05 were considered significant: *$p<0.05$. Mean data from 3 healthy donors are presented, and error bars represent SEM.

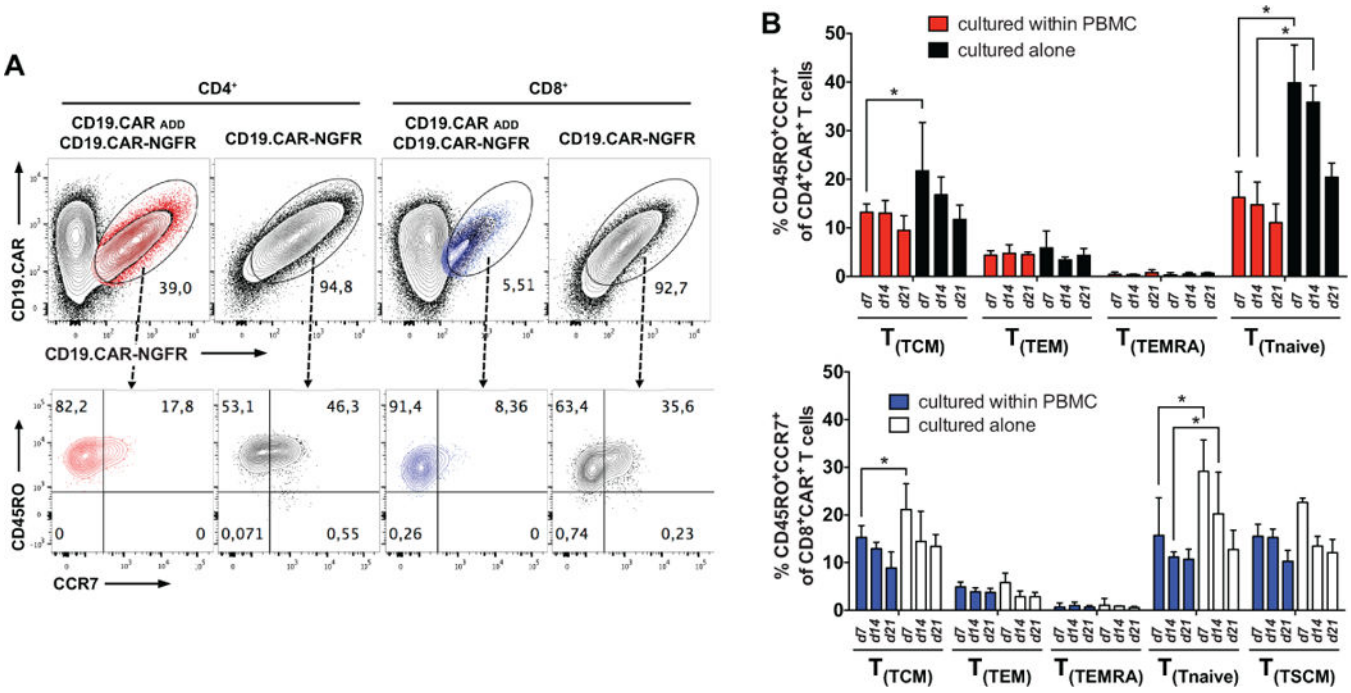

FIGURE 7. T-cells with T_{CM} and T_{EM} phenotypes dominate all T_{SUBSET}–derived populations during culture

CAR-modified T-cell subsets were cultured alone or reconstituted into CD19.CAR modified, subset-depleted PBMC according to Figure 3. (**A**) Representative FACS plots illustrating flow cytometric detection of CCR7 and CD45RO expression on days 7, 14 and 21 post initial activation of T_{SUBSET}-derived ($T_{(TSUBSET)}$) populations (cultured alone) and of T_{SUBSET}-derived ($T_{(TSUBSET)}$) populations within the relevant PBMC-T_{SUBSET} preparation (cultured within PBMC): (**B**) Results for T_{CM} phenotype ($CCR7^+CD45RO^+$) at indicated time-points (days 7, 14 and 21) for all subsets of $CD4^+CAR^+$ and $CD8^+CAR^+$ T-cells. Data from T_{SUBSET}–derived ($CD4^+$CD19.CAR-$NGFR^+$ cultured alone: black bars; $CD8^+$CD19.CAR-$NGFR^+$ cultured alone: white bars versus $CD4^+CD19.CAR^+$ cultured within PBMC preparations: red bars; $CD8^+CD19.CAR^+$ cultured within PBMC preparations: blue bars) were analyzed using paired t-test, after verifying Gaussian distribution with the Kolmogorov-Smirnov test. p-values ≤ 0.05 were considered significant: *p<0.05. Mean data from 3 healthy donors are presented, and error bars represent SEM.

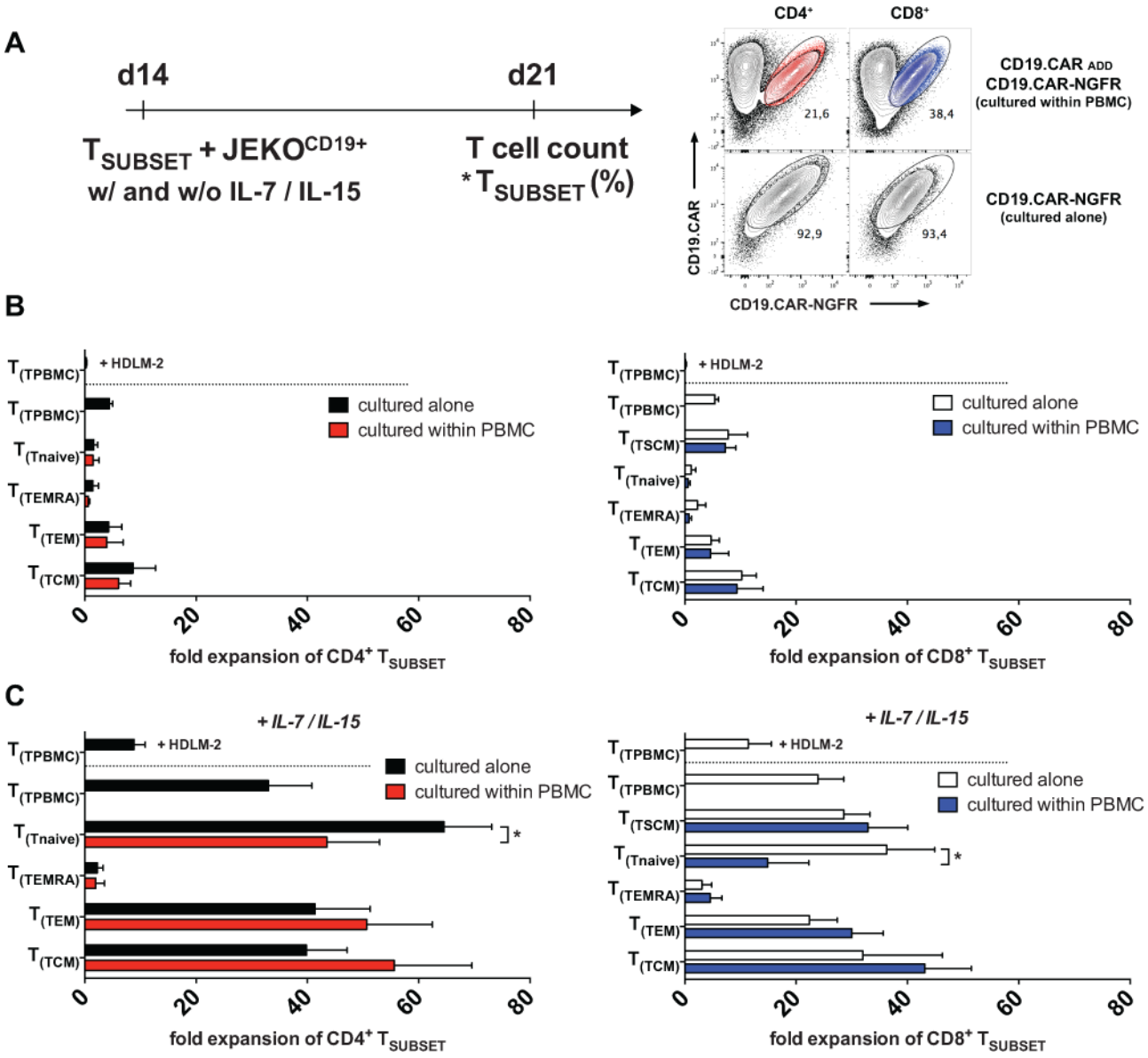

FIGURE 8. Proliferation of CD19.CAR-modified $T_{SUBSETS}$ cell cultured alone or expanded within bulk PBMC in response to CAR stimulation

CAR-modified T_{SUBSET} were cultured alone or reconstituted into CD19.CAR modified, subset-depleted PBMC according to Figure 3. (**A**) Each CD3/28-expanded transduced T_{SUBSET}-derived population cultured alone or within bulk PBMC were stimulated via the CAR using vital $CD19^+$ JEKO cells in the presence or absence of exogenous cytokines (IL-7 and IL-15) at a stimulator to responder ratio of 10:1 14 days after the initial CD3/28 activation. The frequency of each subset was measured by co-staining with antibodies to NGFR and to the spacer/hinge region of the CD19.CAR at assay initiation and post 7 days of consecutive expansion. (**B and C**) T_{SUBSET} expansion (measured as fold increase) was analyzed for each cell subset between days 14 and 21 after stimulation with $CD19^+$ JEKO cells on day 14 in the absence (**B**) or presence (**C**) of exogenous cytokines (IL-7 and IL-15). Data from T_{SUBSET}–derived ($CD19.CAR\text{-}NGFR^+$ cultured alone versus cultured within

PBMC preparations) were analyzed using paired t-test, after verifying Gaussian distribution with the Kolmogorov-Smirnov test. p-values ≤ 0.05 were considered significant: *p<0.05. Mean data from 3 healthy donors are presented, and error bars represent SEM.

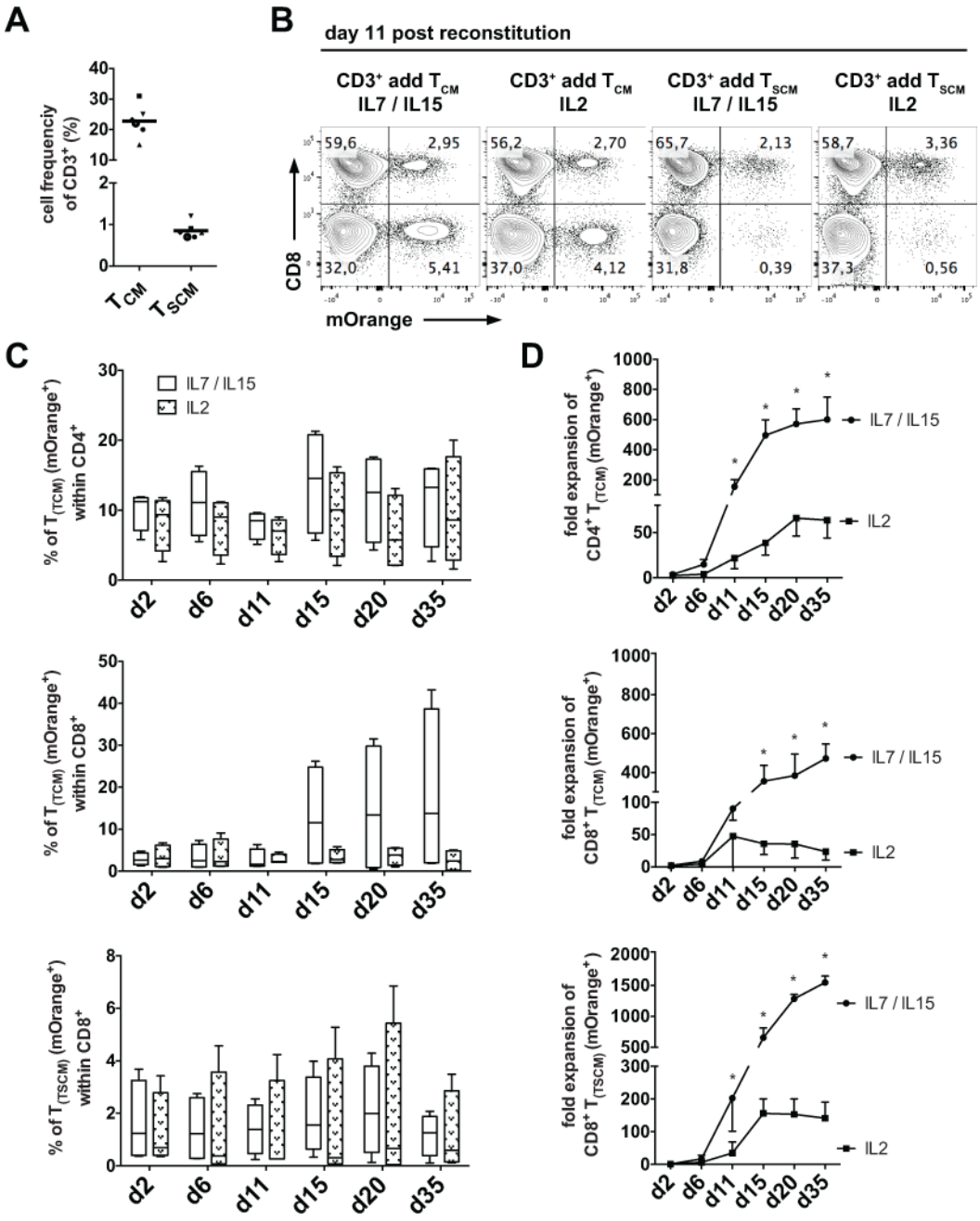

FIGURE 9. A combination of IL-7 and IL-15 increases the yield of T_{SCM} and T_{CM} derived T-cells compared to IL-2

T_{CM} and T_{SCM} were FACSort-depleted from PBMC, activated with CD3 and CD28 antibodies in the presence of either IL-2 (50IU/mL) or IL-7 and IL-15 (each at 10ng/mL) and transduced on day 2 with a retroviral vector encoding mOrange. mOrange$^+$ T_{CM} and T_{SCM} were reconstituted on day 3 to the respective T_{SUBSET}-depleted PBMC. The medium and cytokines were changed every 3 days during culture or when passaging the T-cells for splitting during expansion. (**A**) Shows the frequency of T_{SCM} and T_{CM} in PBMC. (**B**) Representative plot showing the frequency of mOrange-positive T_{CM}-derived ($T_{(TCM)}$) and T_{SCM}-derived ($T_{(TSCM)}$) populations in reconstituted cultures on day 11. Cells were stained

for CD3, CD4 and CD8. (**C**) Frequencies of reconstituted $CD4^+$ T_{CM} (upper graph), $CD8^+$ T_{CM} (middle graph) and $CD8^+$ T_{SCM} (lower graph) during expansion from day 2 to 35 of culture in either IL-2 or IL-7 and IL-15 (T_{CM}-derived: $T_{(TCM)}$; T_{SCM}-derived: $T_{(TSCM)}$). (**D**) Expansion within the bulk population of reconstituted $CD4^+$ T_{CM} (upper graph), $CD8^+$ T_{CM} (middle graph) and $CD8^+$ T_{SCM} (lower graph) measured as fold increase of $mOrange^+$ T-cells over 35 days of culture in IL-2 or IL-7/15 (T_{CM}-derived: $T_{(TCM)}$; T_{SCM}-derived: $T_{(TSCM)}$). Data were analyzed using repeated measures 2-way ANOVA, after verifying Gaussian distribution with the Kolmogorov-Smirnov test. p-values ≤ 0.05 were considered significant: *$p<0.05$. Mean data from 4 healthy donors are presented.